Probabilistic seismic hazard maps for the sultanate of Oman

Nat Hazards (2012) 64:173–210
DOI 10.1007/s11069-012-0232-3

ORIGINAL PAPER

Probabilistic seismic hazard maps for the sultanate of Oman

I. El-Hussain · A. Deif · K. Al-Jabri · N. Toksoz · S. El-Hady · S. Al-Hashmi · K. Al-Toubi · Y. Al-Shijbi · M. Al-Saifi · S. Kuleli

Received: 31 December 2011 / Accepted: 20 May 2012 / Published online: 14 June 2012

Abstract This study presents the results of the first probabilistic seismic hazard assessment (PSHA) in the framework of logic tree for Oman. The earthquake catalogue was homogenized, declustered, and used to define seismotectonic source model that characterizes the seismicity of Oman. Two seismic source models were used in the current study; the first consists of 26 seismic source zones, while the second is expressing the alternative view that seismicity is uniform along the entire Makran and Zagros zones. The recurrence parameters for all the seismogenic zones were determined using the doubly bounded exponential distribution except the zones of Makran, which were modelled using the characteristic distribution. Maximum earthquakes were determined and the horizontal ground accelerations in terms of geometric mean were calculated using ground-motion prediction relationships developed based upon seismic data obtained from active tectonic environments similar to those surrounding Oman. The alternative seismotectonic source models, maximum magnitude, and ground-motion prediction relationships were weighted and used to account for the epistemic uncertainty. Hazard maps at rock sites were produced for 5 % damped spectral acceleration (SA) values at 0.1, 0.2, 0.3, 1.0 and 2.0 s spectral periods as well as peak ground acceleration (PGA) for return periods of 475 and 2,475 years. The highest hazard is found in Khasab City with maximum SA at 0.2 s spectral period reaching 243 and 397 cm/s^2 for return periods 475 and 2,475 years,

I. El-Hussain (✉) · A. Deif · S. Al-Hashmi · K. Al-Toubi · Y. Al-Shijbi · M. Al-Saifi
Earthquake Monitoring Center, Sultan Qaboos University, Muscat, Oman
e-mail: Elhussain@squ.edu.om

A. Deif · S. El-Hady
Earthquake Department, National Research Institute of Astronomy and Geophysics, Helwan, Egypt

K. Al-Jabri
Department of Civil and Architectural Engineering, Sultan Qaboos University, Muscat, Oman

N. Toksoz · S. Kuleli
Massachusetts Institute of Technology, Cambridge, MA, USA

S. El-Hady
Faculty of Earth Science-Geophysics Department, King Abdulaziz University, Jeddah, Saudi Arabia

respectively. The sensitivity analysis reveals that the choice of seismic source model and the ground-motion prediction equation influences the results most.

Keywords Oman · Probabilistic seismic hazard · Logic tree · Deaggregation

1 Introduction

The deformation associated with Oman Mountains range (Johnson 1998; Kusky et al. 2005) and the high active tectonic zones surrounding the Arabian Plate (Fig. 1) makes Sultanate of Oman prone to earthquake activities, although in low rate. The seismotectonic settings around Oman strongly suggest that large earthquakes are possible, particularly along the Arabian plate boundaries and can significantly produce damaging effect to structures in Oman. With exception of the Oman Mountains earthquakes, major earthquake sources are not inside of the Sultanate. The most effective way to reduce disasters caused by earthquakes is to estimate the seismic hazard and to disseminate this information for use to improve building design and construction. The current study is, in particular, concerned with obtaining an estimate of the ground-motion parameters in Oman for the purpose of earthquake-resistant design or seismic safety assessment.

Randomness in seismic hazard assessment arises out of aleatory variability and epistemic uncertainty. In the current study, PSHA is performed utilizing CRISIS 2007 software (Ordaz et al. 2007). The effect of the aleatory variability due to truly random effect is directly incorporated into the calculations of PSHA to determine annual exceedance frequencies of different amplitudes of ground motion. This is done through the integration of the corresponding probability density functions within specified standard deviations. Modern PSHA studies use the "logic tree" approach Coppersmith and Youngs (1986) to handle the epistemic uncertainty.

Hazard maps showing spectral acceleration values at 0.1, 0.2, 0.3, 1.0 and 2.0 s spectral periods as well as peak ground acceleration (PGA) for return periods of 475 and 2,475 years (equivalent to 10 and 2 % probability of exceedance in 50 years, respectively) are presented. The current study includes a sensitivity analysis to reveal how the variations in the alternative parameter assessments influence the results.

2 Seismotectonic setting of sultanate of Oman and its surrounding

Oman occupies the southeastern part of the Arabian plate, which shows all tectonic margin types in close proximity (Fig. 1). Divergent boundaries are evident to the west and south in the spreading centres of the Red Sea and the Gulf of Aden. Convergent margin lies along the Zagros-Bitlis zone, where continental collision has given rise to the Turkish–Iranian Plateau. The remainder of the convergent margin of the Arabian plate is defined by the Makran subduction zone, where the Arabian plate subducts beneath the Eurasian plate (Farhoudi and Karig 1977; Bayer et al. 2006). The strike-slip Dead Sea fault zone bounds the plate in the northwest. Another transform boundary with the Indian plate exists to the southeast, at Owen fracture zone, which is the oldest and least active tectonic margin of the Arabian plate (Johnson 1998; Vita-Finzi 2001; Fournier et al. 2008). Kusky et al. (2005) indicated the presence of some active tectonic structures in Oman Mountains. The scarcity of the geologic features information of northern Oman makes it difficult to define precisely the nature of the structures of Oman Mountains.

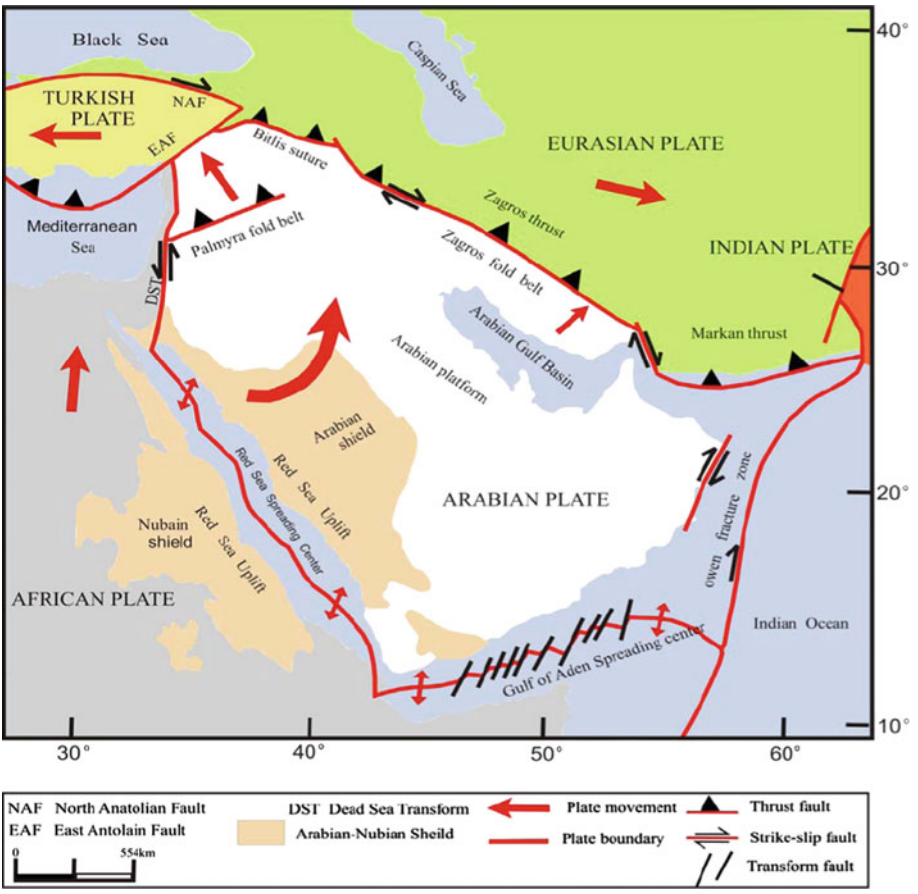

Fig. 1 Major tectonic elements surrounding the Arabian plate. *DST* dead sea transform, *EAF* east anatolian fault, *NAF* north anatolian fault (Bosworth et al. 2005)

Most of the seismic activity is confined to the boundaries of the Arabian plate (Fig. 2). The interior of the plate may be regarded, therefore, as a stable cratonic region (Johnson et al. 1994; Fenton et al. 2006; Aldama et al. 2009). Smaller earthquake cluster is represented by the local seismicity at the north of Oman Mountains. A few scattered background events occured within the Arabian plate and the Sea of Oman. Figure 3 shows the focal mechanisms of the earthquakes associated with the tectonic units of the region (Reilinger et al. 2006). It is evident that the focal mechanisms of large earthquakes are consistent with the regional kinematics. The seismotectonic characteristics of the active regions that might affect Oman are briefly discussed below.

2.1 Oman Mountains

The Oman Mountains are located in northern Oman exhibiting many features consistent with active tectonics (Johnson 1998; Kusky et al. 2005). In addition to the field evidences of active faulting, evidence of seismic activity is also present (Ambraseys et al. 1994; Kusky et al. 2005; Musson 2009). All of the devastating earthquakes that occurred in or

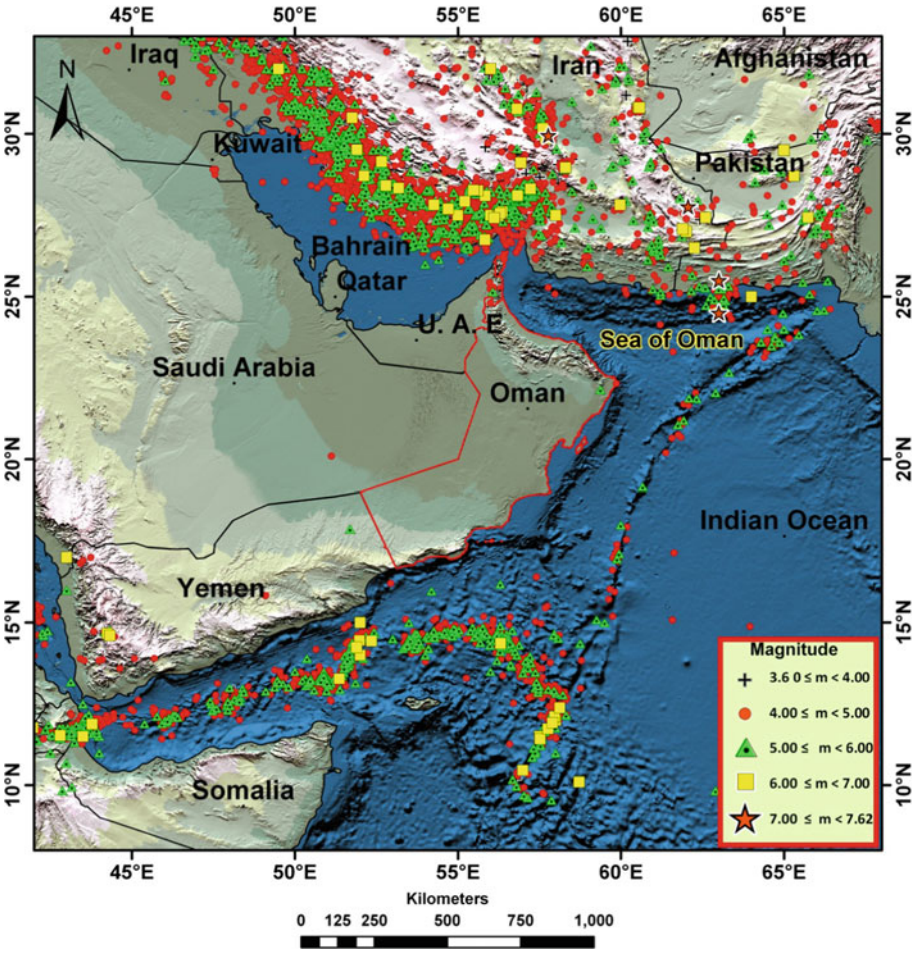

Fig. 2 Instrumental seismicity of Oman and its surrounding in terms of moment magnitude in the period from 1904 to 2008

near the Sultanate of Oman are historical ones. They extend back to 879 AD including events that occurred near Sohar region in 879 (Ambraseys et al. 1994), the earthquake that damaged Qalhat in northern Oman in 1483 (Aubin 1973; Ambraseys et al. 1994; Musson 2009). The earthquake occurred in 1883 (Ambraseys et al. 1994), which is strongly felt at the southern part of the mountains in Muscat and Nizwa, in the vicinity of which nine villages were destroyed and ground deformation was observed.

The instrumental seismicity (Fig. 2) in the Oman Mountains seems to be clustered at its northern part. The historical event in 1,883 near Nizwa (Ambraseys et al. 1994) supports the possibility of the occurrence of moderate events along the entire zone (Fig. 4). Two earthquakes with magnitudes 4.5 and 5.1 occurred on 10 and 11 March 2002. These two events were felt broadly in northern Oman and UAE. Focal mechanism solution for the larger event shows normal faulting with strike-slip component, which is consistent with the large-scale tectonics of the region (Rodgers et al. 2006).

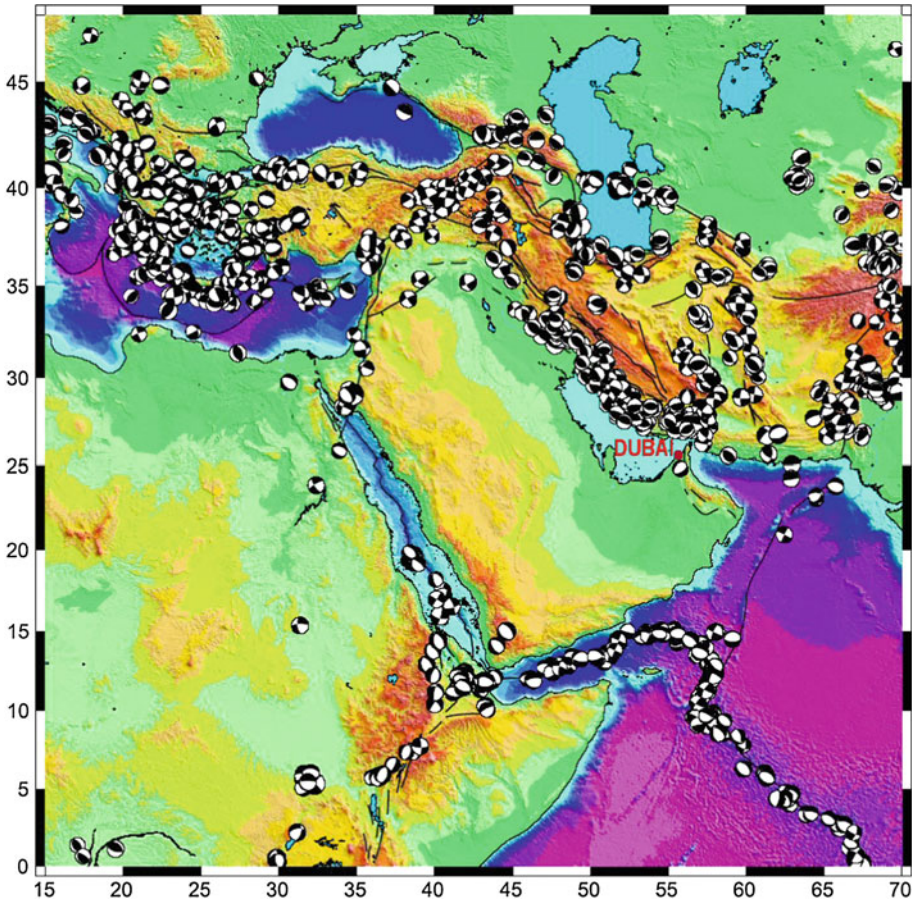

Fig. 3 Regional seismicity indicated by the focal mechanisms of earthquakes (Reilinger et al. 2006)

2.2 Zagros fold-thrust belt

The Zagros fold-thrust belt (Fig. 1) is a linear, asymmetrical NW–SE phanerozoic folding, extending for about 1,500 km from eastern Turkey to Oman (Jackson and McKenzie 1984; Berberian 1995; Hessami et al. 2003). This collision between the Arabian and the Eurasian Plates is over an area of 200–300 km wide series of blind thrust faults covered by folded Phanerozoic sedimentary rocks, with strike-slip faults accommodating internal deformation. The active Mountain Front Fault (MFF), High Zagros Fault (HZF) and Main Zagros Fault (MZF) are major segmented reverse faults, whose seismogenic and morphologic signature is recognized throughout the Zagros fold-thrust belt (Fig. 5). This Pliocene fold-thrust belt is currently undergoing approximately 10 mm/year shortening in the southeast and 5 mm/year in the northwest (Allen et al. 2004; Vernant et al. 2004). The 6–15-km-thick Phanerozoic cover is folded, producing active anticlinal uplift and synclinal subsidence (Berberian 1995). This surface deformation may be used to infer the locations of the dominant blind thrust faults.

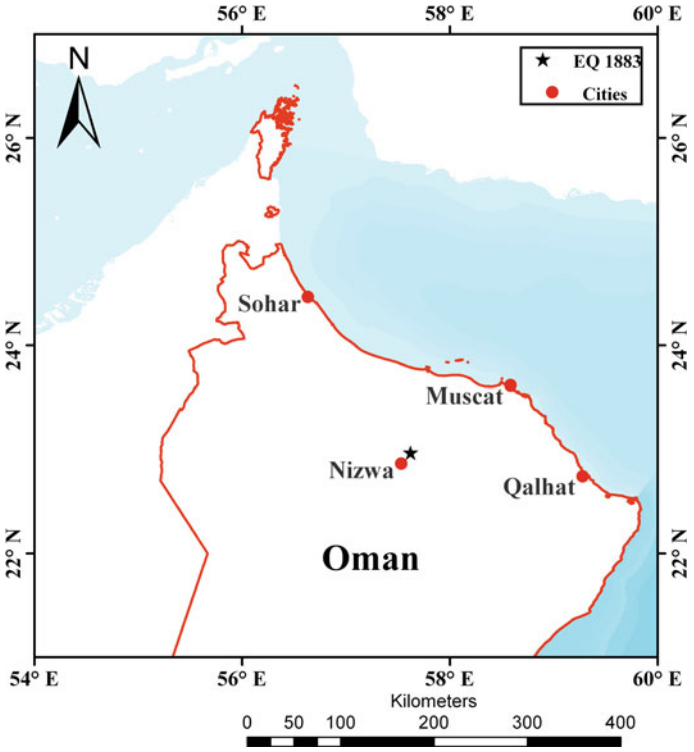

Fig. 4 Location of 1,883 earthquake in Northern Oman

The seismic activity along Zagros zone is relatively high (Fig. 2). This activity occurs in a wide seismogenic belt, which suggests that, the plate border is a zone of deformation instead of single line. Moderate to large earthquakes frequently occur but rarely exceed $M_W = 7.0$. Recently determined focal depths (8–14 km) imply that moderate to large earthquakes occur in the uppermost part of the Arabian basement (Ni and Barzangi 1986; Baker et al. 1993; Hessami et al. 2001; Hatzfeld et al. 2010). Focal mechanism solutions (Fig. 3) show high-angle thrust faults (40°–50°) parallel to the trend of the fold axes (Nowroozi 1972; Jackson and McKenzie 1984; Gillard and Wyss 1995; Reilinger et al. 2006). Focal mechanism solutions along the transverse faults show steeply dipping strike-slip faults with minor dip-slip components (Hessami et al. 2006).

2.3 Gowk fault

Shortening that is not taken up in the Zagros due to the convergence between Arabian and Eurasian plates is expressed as N–S right lateral shear between central Iran and Afghanistan. This shear is expressed in major N–S right lateral fault systems, the most active among them is Gowk fault (Fig. 5). Many moderate to large earthquakes have been occurred on Gowk fault (Zone No. 12). A maximum magnitude as large as 8.0 can be occurred on this fault Berberian and Yeates (1999).

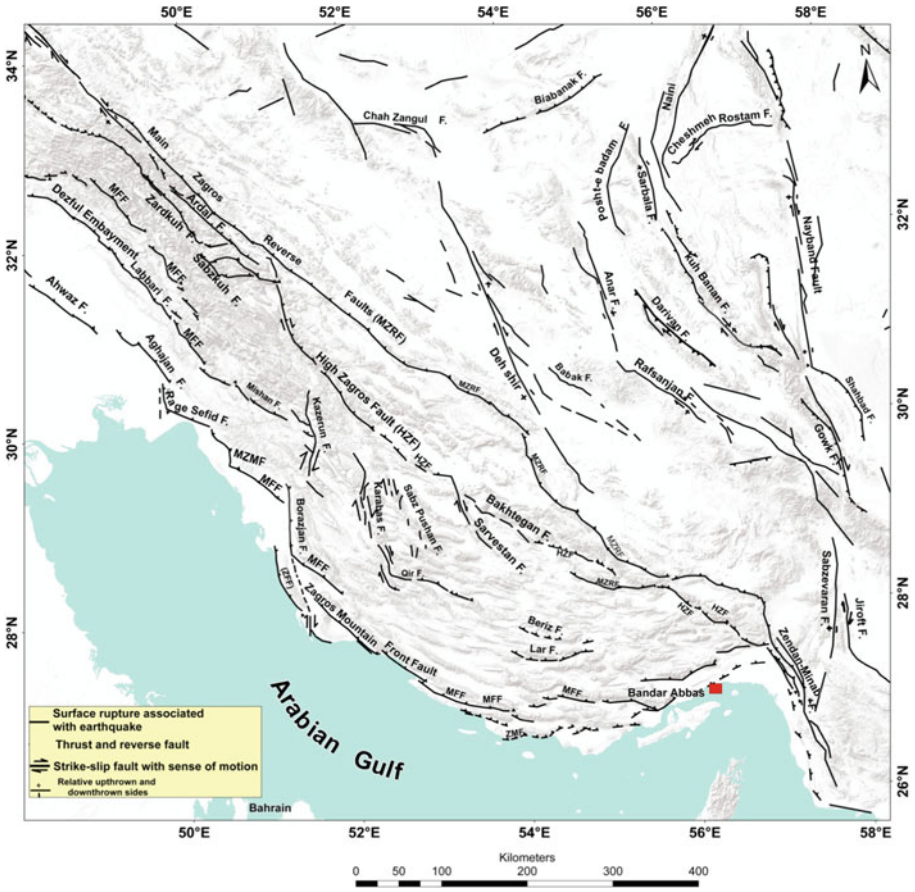

Fig. 5 The main fault zones of Zagros thrust belts (modified after Hessami et al. 2003)

2.4 Makran subduction zone

The Makran subduction zone (Fig. 1) is composed of a large sedimentary prism accreted during the Early Cretaceous (Byrne et al. 1992). The Makran accretionary wedge stretches from Iran to central Pakistan (Schluter et al. 2002). It has been formed by the subduction of the oceanic portion of the Arabian Plate beneath Eurasia and is built up by sediments scraped off the Arabian Plate since early Tertiary (Kopp et al. 2000). Stoneley (1974) was the first to propose a subduction zone along the Makran zone. Later, Shearman (1977) and Farhoudi and Karig (1977) presented data to support this hypothesis. The distance between the volcanic arc and the deformation front is approximately 400 km in western Makran and grows to nearly 600 km in eastern Makran (Fig. 6).

The modern Makran accretionary prism has developed since Late Miocene (Platt et al. 1988) and is still propagating seaward at a rate of $\sim$10 mm/year. Two features make this accretionary wedge unusual: (1) the sediment thickness on top of the oceanic crust is extremely high (at least 6 km), and (2) the dip angle of subduction is extremely low, $\sim$5°, (Byrne et al. 1992; Carbon 1996).

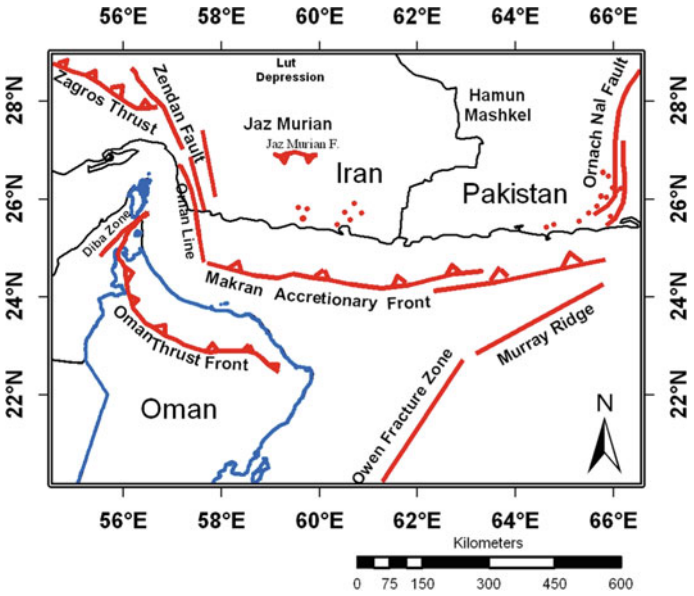

Fig. 6 The Oman thrust front and the Zone of Tectonic Subduction in the Northern Arabian Sea

The most notable earthquake in Makran zone is the 28 November 1945 of $M = 8.1$, a tsunamigenic event that killed 4,000 according to Dunbar et al. (2002) and about 300 according to Ambraseys and Melville (1982). The tsunami was recorded along the coasts of Iran and in Muscat (ASC 2003; Pararas-Carayannis 2004). With the exception of 1,483 ill-located earthquake with magnitude 7.8, all large earthquakes are reported to have occurred in the eastern section of Makran zone. Kukowski et al. (2000) provided an explanation of why the Eastern Makran is entirely separated from the Western section. This suggests that a single event rupturing the entire Makran zone is improbable. Therefore, in the seismogenic model provided by the current authors, western Makran is preferred to be separate seismogenic zone having the possibility of producing large earthquakes.

2.5 Transition between Zagros and Makran

Geology and recent GPS measurements indicate that about 15 mm/year (Peyret et al. 2009) of relative motion in N10°E direction in this transition zone is accommodated by two major fault systems: Minab-Zendan (MZFS) and Jiroft-Sabzevaran fault systems (JSFS) (Fig. 5). For both fault systems, the elastic deformation spreads over shear zones that are several tens of kilometres wide. Historical (Ambraseys and Melville 1982; Musson 2009) and instrumental seismicity (e.g. Gholamzadeh et al. 2009), as well as microseismic activity (Yamini-Fard et al. 2007), appear to be essentially limited to the Zagros domain. Seismicity appears to neither be associated with the Minab-Zendan nor Jiroft–Sabzevaran faults, suggesting that the transition between the Zagros collision and the Makran subduction is not a sharp transform fault. The seismogenic potentials of these two faults are not as great as those comprising the major margins of the Zagros and the Makran. However, their proximity to sites within the northeastern Oman means that these fault systems may contribute to the seismic hazard and must be included within the developed seismotectonic source model.

Peyret et al. (2009) stated that the strain localization on the Minab-Zendan fault system, without transfer within the inner Makran, associated with the lack of historical and instrumental seismicity, indicates that about 2 m of elastic strain has probably been accumulated for the last two centuries. It suggests that this fault system is likely at the end of its interseismic recurrence cycle. Hence, they claim that seismic hazard on this zone is high and that an earthquake of magnitude in the vicinity of 7.0 is pending.

2.6 Owen fracture zone

Owen fracture zone (Fig. 1) is 1,100-km-long transform fault separating the Arabian plate from the Indian plate. The Arabian and Indian plates are colliding with the southern edge of Eurasia but the Arabian plate is moving slightly faster than the Indian one. The rate of differential motion along this fracture zone is one of the slowest among major plate boundaries (3 mm/year) (DeMets 2008). Plate motion models (e.g. McKenzie and Sclater 1971; Chase 1978; Minster et al. 1974; Minster and Jordan 1978; Quittmeyer and Kafka 1984) assumed right lateral slip along Owen fracture zone. Earthquake focal mechanisms show that the sense of motion along Owen fracture is right lateral strike-slip motion (Fig. 3). The seismicity of Owen zone changes its orientation at the northern part to coincide with Murray ridge (Figs. 2, 6).

2.7 Gulf of Aden

The seismicity of the Gulf of Aden indicates a tensile stress regime as the main force (Fig. 2). Transform faults along the central axis of the Gulf of Aden are characterized by linear NE trending. The most spectacular one is Alula Fartak trench where central ridge is offset a distance of 160 km. Earthquake distribution is exhibiting a well demonstration of this transform fault (Fig. 2). Earthquakes associated with this trench show strike-slip mechanisms characteristic of oceanic transform (Sykes and Landisman 1964). Most of the seismicity of the Gulf is confined around the rift axis and its transform faults. As one moves from the central axis of the Gulf of Aden, seismicity level decreases drastically and thus the seismicity cannot be stationary from the space and time point of view.

2.8 Yemen

Yemen has been affected by earthquakes along the Red Sea and its coastal tract, as well as inland. Ma'rib Dam earthquake, in the year 460 (Ambraseys et al. 1994), is the oldest available information of destructive earthquakes in Yemen. Dhamar earthquake (31 December 1982 with Ms 5.7), which resulted in wide destruction, loss of lives and surface rupture, occurred in an area of recent volcanic activity that characterizes much of the southwestern margin of the Arabian Plate. This earthquake was characterized by high level of aftershock activity, including a widely felt event with a damaging effect with mb 5.1 (Alsinawi and Al-Salim 1985; Langer et al. 1987; Plafker et al. 1987).

3 Input for PSHA in Oman

The PSHA was first introduced by Cornell (1968); although many modifications have been made to the process (e.g. McGuire 1978; Bender and Perkins 1987), the basic elements of the calculations remain unchanged. PSHA is widely adopted and is considered as

seismology's most valuable contribution to earthquake hazard assessment (Giardini et al. 1999; Abrahamson and Bommer 2005; Deif et al. 2009). Input parameters needed for performing a PSHA following the Cornell–McGuire approach (Cornell 1968; McGuire 1976; Reiter 1990) are:

1. An earthquake catalogue, which is used to derive recurrence rates and to estimate the maximum possible earthquake for each seismic zone with potential hazard on Oman.
2. A seismotectonic source model, which defines faults and/or areal zones of equal seismic potential.
3. The seismicity recurrence characteristics for the seismic sources, where each source is described by an earthquake recurrence relationship. A maximum or upper-bound earthquake is chosen for each source, which represents the largest event to be considered.
4. A predictive ground-motion model describes the attenuation of amplitudes of ground motion as a function of distance and magnitude. Different models are constructed for different frequencies and local site conditions. Below, we describe how these input parameters were derived for Sultanate of Oman.

Considering the lack of the seismotectonic studies in the Arabian Plate and the short period for which earthquake data are available, there is therefore an element of uncertainty in identifying the seismogenic zones.

3.1 Earthquake catalogue

Preparing a reliable, as long as possible, and homogenous earthquake catalogue represents the starting point for any seismic hazard assessment study regardless of the approach adopted. There is no unique catalogue for a given territory but usually a heterogeneous set of catalogues (historical, instrumental, local, global, etc.), which are not always comparable, and may require different tools of analysis. For the purpose of characterizing the activity rates of the Oman seismic sources, a catalogue was compiled using information from several seismic sources. These are:

- Preliminary Determination of Epicenters (PDE), on line bulletin provided by the National Earthquake Information Center (NEIC) (http://earthquake.usgs.gov/earthquakes/);
- The International Seismological Center (ISC) online bulletin (http://www.isc.ac.uk/);
- EHB (Engdahl et al. 1998) catalogue updated to 2006 from the webpage of the ISC;
- HRVD which is operated now as Global Centroid-Moment-Tensor projectat (GCMT), Lamont Doherry Earth Observatory (LDEO) http://www.globalcmt.org/CMTsearch.html earthquake data bulletins;
- Ambraseys Publications, Ambraseys and Melville (1982); Ambraseys et al. (1994); Ambraseys and Bilham (2003);
- Bulletins of Earthquake Monitoring Center (EMC) at Sultan Qaboos University (SQU), Oman.

All available data from the above catalogues were gathered and compiled into one comprehensive catalogue. The catalogue is built by merging historical and instrumental data. In addition, the following studies on specific events or region were also consulted to gather additional information regarding earthquakes of considerable size (Berberian 1973; Quittmeyer 1979; Jackson and Fitch 1981; Alsinawi 1983; Jackson and McKenzie 1984; Baker et al. 1993; Berberian 1995; Berberian and Yeates 1999; Berberian et al. 2001; Maggi et al. 2002; Talebian and Jackson 2004; Walker et al. 2005; Rodgers et al. 2006; Al Marzooqi et al. 2008).

Due to the fact that publications of different international and local agencies were used to compile the current catalogue, any duplication in the resultant catalogue was removed. If more than one location entry is available for a single earthquake, priority was given to the published and international data, since it is more accurate due to the availability of more stations all over the world, longer than the available local catalogue, and the additional work of relocating such events. Thus, for earthquakes occurred before 1964, Ambraseys et al. publications are selected. For earthquakes that occurred after 1964, data from studies on specific events or region are selected as the most reliable followed by Ambraseys et al. publications, EHB, ISC, PDE and EMC, respectively.

With respect to earthquake magnitude, for earthquake occurred before 1964, priority was given to Ambraseys publications followed by ISC and PDE, respectively. For earthquakes occurred after 1964, priority was given to Harvard moment magnitude (M_W), if available, followed by Ambraseys publications, ISC and PDE, respectively. Priority considering the magnitude type was taken according to the following succession: moment magnitude (M_W), surface wave magnitude (M_S), body wave magnitude (m_b) and local magnitude (M_L), respectively.

The initial catalogue was compiled for a spatial region spanning from 42° to 66°E and 10° to 32°N and included all events having an assigned magnitude of 3.0 and above on any magnitude scale. The catalogue covers the time period from 734 up to January 2008. The compiled catalogue comprises a total of about 4,593 earthquakes.

To ensure the catalogue magnitude homogeneity, all events for which M_W were not reported were converted into this scale. Conversion of multiple magnitude measures to a single, representative magnitude is performed using empirical relationships developed directly from the various magnitude measures in the compiled catalogue (Fig. 7). Many magnitude conversion relations are available worldwide (e.g. Ambraseys and Free 1997; Grunthal and Wahlstrom 2003). Figure 8 shows good agreement between the M_S–M_W conversion equation of this study and that of Ambraseys and Free (1997) for Europe along the entire range of interest.

The M_W was chosen because it is the most reliable magnitude scale. Moreover, most of the ground-motion prediction models used in this study are expressed in terms of M_W. The spatial distribution of the instrumental compiled catalogue, using a consistence M_W magnitude scale, is shown in Fig. 7.

Dependent events in the catalogue (i.e. foreshocks and aftershocks) were declustered. The process consisted of the definition of a temporal and spatial windows adapted to each range of magnitude. All earthquakes situated inside the window defined around a main shock were considered as dependent events. Windows of Gardner and Knopoff (1974) were applied and 2,575 dependent events were removed from the original catalogue with 5.92 % contribution to the total moment released.

To model the seismicity in each zone, knowledge of the magnitude of completeness, Mc, is required. Although any event having an assigned magnitude greater than 3.0 was initially included into the base catalogue, for most of the period spanned by the catalogue, the level of completeness is significantly greater than this level. The procedure of Stepp (1972), which based upon the change of the slop of the cumulative seismicity with time, is used to identify the completeness levels of the catalogue. The catalogue is regarded as being complete above M_W 3.0 from 2001 onward, M_W greater than 4.0 from 1987, M_W greater than 4.8 from 1965, M_W greater than 5.6 from 1923, M_W 6.0 from 1910, and M_W greater than 7.0 from 1,800.

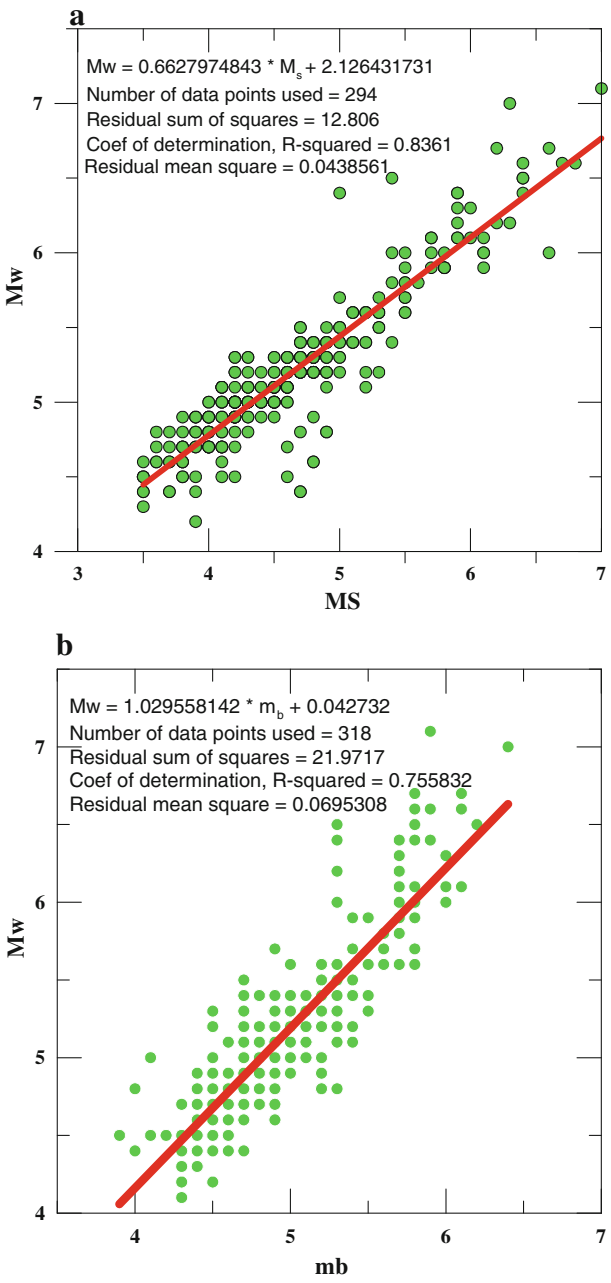

Fig. 7 Conversion of (**a**) surface wave magnitude (M_s) and **b** body wave magnitude (m_b) into moment magnitude (M_w)

3.2 Seismotectonic source models

The seismic sources are shown as map representations of lines (fault sources) and area source zones. The seismicity within these zones is assumed to be uniform in terms of the type and distribution of earthquakes. Thus, the seismic activity of the source is

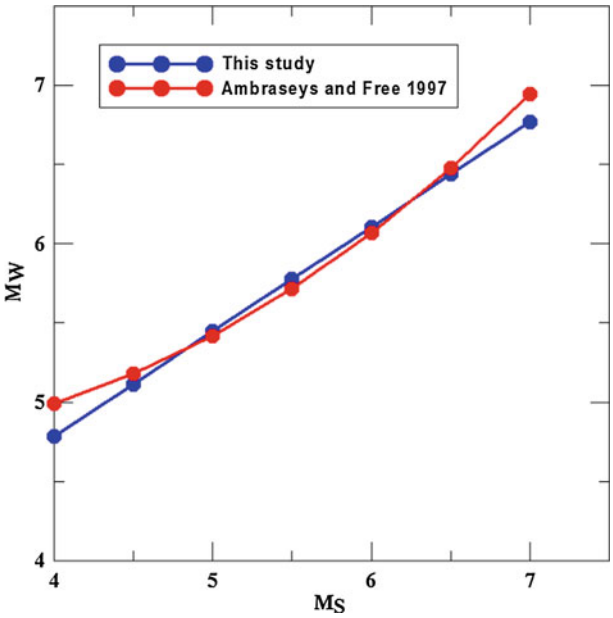

Fig. 8 Comparison between the M_S–M_W conversion equation of this study and that of Ambraseys and Free for Europe (1997)

characterized by a single earthquake generating process, and the earthquakes have an equal probability of occurring at any point within the seismic zone. The defined geographic distribution of seismic sources and the specification of all source characteristics required for the seismic hazard analysis are termed seismotectonic source model. Integration of geology, structure, present-day tectonics, seismicity and focal mechanisms guided the modelling of the seismogenic zones of the current study.

3.2.1 Seismic source zones

For the hazard computation of the current study, two seismogenic source models were used to account for the epistemic uncertainty. The first model (Fig. 9) is developed by the current authors and based upon the seismotectonic setting briefly summarized above and previously published studies (e.g. Berberian 1995; Aldama et al. 2009), while the second is Erdik et al. (2008) model for the northern part of the studied area, which attempts to capture the major tectonic features of the region (Fig. 10).

The first seismotectonic model constitutes 24 distinct seismic zones (Table 1) and was constructed taking into consideration all the seismic sources that might affect Oman. Most of the seismic zones in this model are mainly related to the active tectonics in the Zagros thrust belt, Makran, transition zone between Zagros and Makran zones, Owen fracture zone, Gulf of Aden, and Oman Mountains. As the location of the concealed blind faults and their slip rates in Zagros fold-thrust belt are difficult to be defined precisely, thus, it is prudent to regard the major seismogenic zones of this region as area zones. The differences in the seismic activity, the active faulting, present-day tectonics, and the surface geology enabled us to divide this belt from northeast to southwest into five main areal seismogenic zones in addition to four strike-slip faults that accommodate the internal deformation (Fig. 9). These five main seismogenic zones are: High Zagros Thrust Belt; Simple Fold

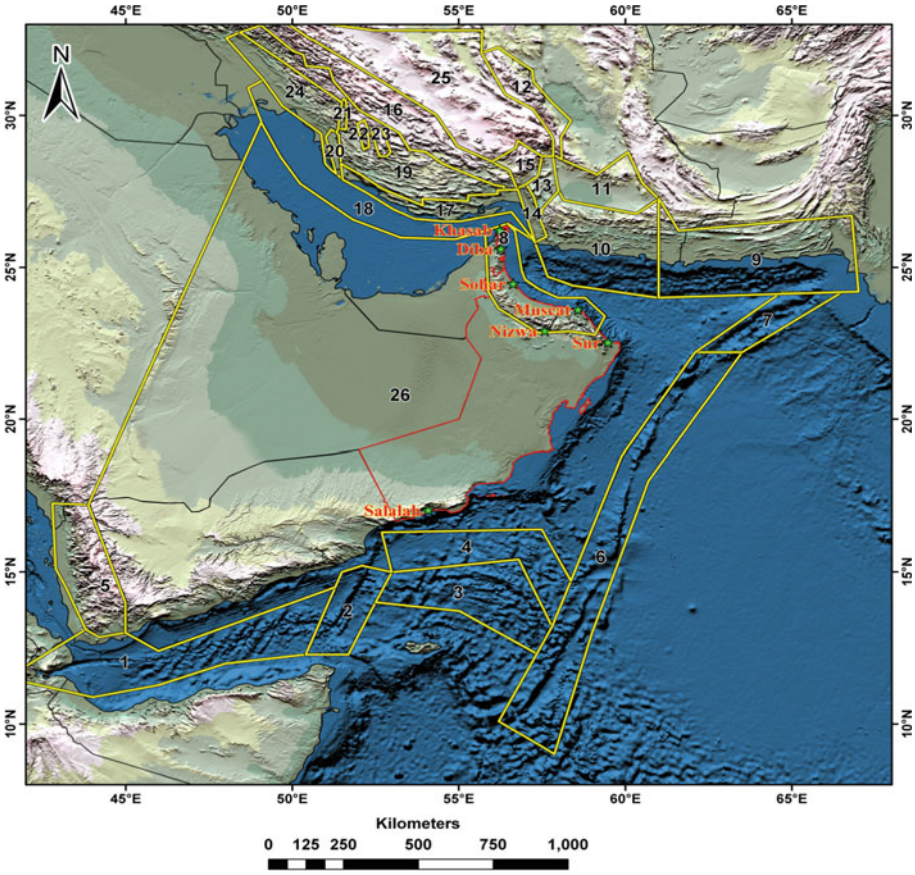

Fig. 9 The first seismotectonic source model for the area of study, the locations of major cities in Oman are also shown

Belt; the Zagros Foredeep; Dezful embayment; and the Arabian Gulf. The four right lateral strike-slip faults are related to Kazerun-Borazjan fault, the Karebas fault, and the Sabz Pushan (Fig. 5). In the current study, the active strike-slip faults in Zagros are modelled as fault sources. The polygons bordering these faults are regions for which the observed seismicity is assumed to be associated with the fault sources.

Makran zone is divided into west and east Makran based upon the dramatic change in the seismicity pattern in these two sections. Owen Fracture zone is divided into Owen and Murray seismic zones due to the change in the fracture trend. The seismicity in the Gulf of Aden is modelled by three main seismogenic zones, Western Gulf of Aden and Eastern Gulf of Aden, which are separated by Alula Fartaq transform fault (Zone No 3). As one moves from the central axis of the Gulf of Aden, seismicity level decreases drastically and thus the seismicity cannot be stationary from the space and time point of view. Therefore, Northeastern Gulf of Aden (Zone No. 4) was selected to represent this lower seismicity level toward the northeastern part of the Gulf of Aden. Yemen zone is included because the 1982 event in Yemen is felt in southern Oman.

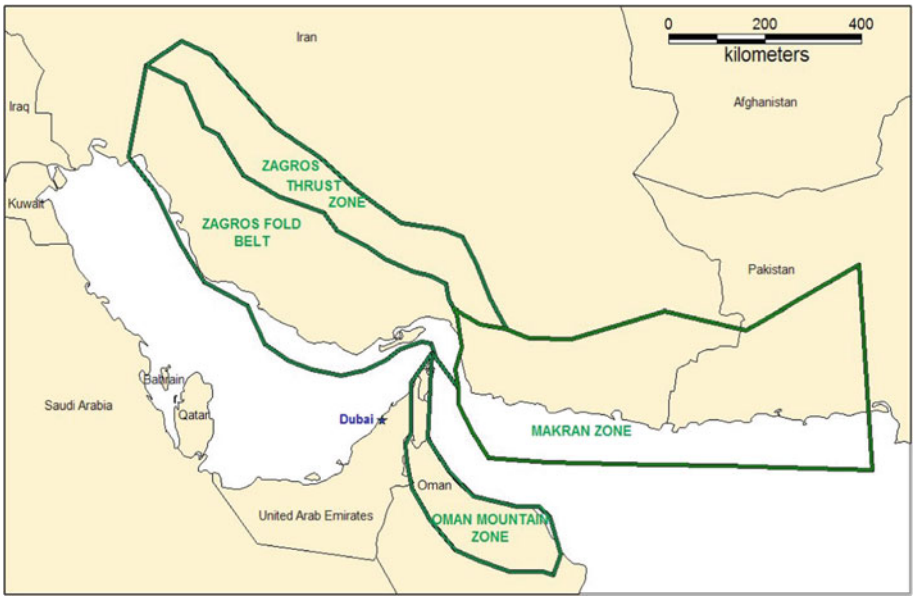

Fig. 10 Erdik et al. (2008) seismotectonic source model for the northern part of the studied area

Table 1 Seismic sources of seismotectonic source model for the PSHA

No.	Source name	No.	Source zone
1	Western Gulf of Aden	14	Minab-Zendan Fault
2	Alula Fartaq Zone	15	Aliabad
3	Eastern Gulf of Aden	16	High Zagros Zone
4	Northeastern Gulf of Aden	17	Zagros Foredeep
5	Yemen	18	Arabian Gulf
6	Owen	19	Zagros Simple Fold
7	Murray zone	20	Borazjan Fault
8	Oman Mountains	21	Kazerun Fault
9	East Makran	22	Karebas Faults
10	West Makran	23	Sabz Pushan Fault
11	Jaz Murian depression	24	Dezful Embayment
12	Gowk fault	25	Iranian Background Zone
13	Jiroft-Sabzevaran fault	26	Arabian background Zone

In addition to the 24 distinct seismic sources, two background seismicity zones were selected to model the floating earthquakes that are located around the studied area. The Iranian background zone includes the central Iran area between the Main Zagros Thrust Fault and the Gowk Fault. The Arabian background zone extends to include the interested part of the Arabian Peninsula and the western part of the Arabian Sea.

3.3 Recurrence parameters

3.3.1 Determination of β and λ values

The seismicity of a seismogenic zone is quantified in terms of the recurrence relationship.

$$\text{Log } N(M) = a - bM \tag{1}$$

where N is the number of earthquakes of magnitude (M) or greater per unit time. The a value is the activity and defines the intercept of the above recurrence relationship (Gutenberg and Richter 1944) at M equal zero. The number of occurrences per year of a hazardous event (e.g. the annual frequency that ground-motion parameter, X, at a site exceeds a specified value x) is defined as the annual frequency and usually denoted as $\lambda(X \geq x)$. The parameter b is the slope, which defines the relative proportion of small and large earthquakes.

While the Gutenberg and Richter 1944 relationship describes the regional occurrence frequency of earthquakes, it fails to represent occurrence of large earthquake on individual faults. This can be attributed to the breakdown of this power law between large and small earthquakes because they are not self-similar processes. This leads to what is called Characteristic earthquakes on active faults. The recurrence parameters of eastern and western sections of Makran subduction zone were taken after Aldama et al. (2009) who modelled them using the characteristic model of Youngs and Coppersmith (1985). These recurrence parameters are listed in Table 2. WSZ1 and WSZ2 are the two likely widths of Makran seismogenic zones considered by Aldama et al. (2009).

The seismic activity in all the remaining seismogenic zones was assumed to be produced according to a doubly bounded exponential distribution (Cornell and Vanmarcke 1969). This is because Gutenberg and Richter (1944) relationship imposes the unrealistic assumption that the maximum potential earthquake for any region under consideration is unbounded and unrelated to the seismotectonic setting. The following truncated exponential recurrence relationship is used:

$$N(\geq M) = \alpha \frac{\exp[-\beta(M - M_{\min})] - \exp[(M_{\max} - M_{\min})]}{1 - \exp[-\beta(M_{\max} - M_{\min})]} \tag{2}$$

where $\alpha = N(M_{\min})$, $M_{\min}$ is an arbitrary reference magnitude; $M_{\max}$ is an upper-bound magnitude where $N\ (m) = 0$ for $M > M_{\max}$; and $\beta = b \cdot \ln 10$. In this form, earthquake frequency approaches zero for some chosen maximum earthquake of a region. The parameters of the doubly bounded exponential distribution were obtained in the current study using the maximum likelihood estimation procedure of Weichert (1980).

In many hazard studies, an overall β value is used to stabilize the results by avoiding undue fluctuations of β particularly in low seismicity zones (Frankel 1995; Frankel et al. 1997; Deif et al. 2009). Where information available for seismogenic zones are insufficient

Table 2 Characteristic seismicity of Makran zones (Aldama et al. 2009)

Zone	Option	$M_{\max}$	$M_{\min}$	M_{char}	σ (M_{char})	Occurrence interval (year)
East Makran	WSZ1	8.3	7.5	8.0	0.25	139
East Makran	WSZ2	8.5	7.8	8.2	0.25	422
West Makran	WSZ1	8.2	7.4	7.8	0.25	121
West Makran	WSZ2	8.4	7.6	8.0	0.25	356

for accurate statistical assessments of the seismicity parameters, the β value indicative of the tectonic characteristics of the region containing these zones is utilized. In such case, the λ values were calculated by fixing the common β values within Weichert's (1980) procedure. This is justified because the seismicity in these zones is very low and the major units are experiencing the same tectonic regime.

For the Arabian stable craton, β is found to be 2.22. This value is close to that of Johnson et al. (1994) who reported a β value of 2.26 as an average over all stable continental regions. The seismicity parameters of all seismogenic zones are listed in Table 3. All the seismogenic zones in Erdik et al. (2008) model including Makran zone were treated as area sources and the recurrence parameters were determined using the doubly bounded exponential model.

3.3.2 Definition of the maximum earthquake for each seismic source

Selection of the maximum earthquake ($M_{\max}$) has a considerable impact on the hazard results, especially at longer return periods (Wiemer et al. 2008). $M_{\max}$ is possibly the most difficult recurrence parameter to assess in the study area because the database in many seismogenic zones is statistically very limited. Therefore, the maximum magnitudes are determined with varying methods depending on the nature the source zone (fault or area source) and robustness of the available seismological database of each zone.

Regression relationships between earthquake magnitude and fault parameters have been developed during the past several decades (e.g. Slemmons 1977; Bonilla et al. 1984; Wells and Coppersmith 1994; Hanks and Bakun 2002). Both geological and historical observations of the rupture history of highly active and carefully investigated faults indicate that faults do not rupture their entire length in a single event, except in unusual structural situations (Allen 1975). A conservative practice is to assume a fraction up to one-half the total length of a fault to rupture in a single event. Along the San Andreas Fault system, this fraction is one-third to two-fifths (Reiter 1990). Slemmons (1982) showed that this fraction of the fault length decreases as the fault length itself decreases. His data set showed that rupture lengths range from about 17 to 33 % of the total fault lengths, with the smaller value typical of faults less than about 200 km long and the larger value typical of faults having lengths of more than 1,000 km.

With exception of Gowk fault with length of about 450 km long, all the fault sources in the current study have lengths less than 200 km. The authors selected a 20 % of the total fault length to represent a conservative fractional length to apply to the studied faults, where 40 % of Gowk fault length is supposed to rupture in a single earthquake. The empirical relationships of Wells and coppersmith (1994) are used to calculate the maximum magnitude for the fault sources when consistent data about the total length and fault type are available (Table 3).

For the remaining area seismic zones with sufficient seismological information, the maximum magnitude was estimated using the statistical procedure of Kijko (2004), using the following equations:

$$M_{\max} = M_{\max}^{\text{obs}} + \int_{M_{\min}}^{M_{\max}} [F_m(m)]^n dm \tag{3}$$

where $Fm(m)$ is the cumulative density function (CDF) of magnitude. From this equation, an estimated value of $M_{\max}$ can be obtained only by iteration. This equation states that $M_{\max}$ is equal to the largest observed magnitude ($M_{\max}^{\text{obs}}$) plus an amount $\Delta = \int_{M_{\min}}^{M_{\max}} [F_m(m)]^n dm$. This

Table 3 Recurrence parameters using doubly bounded exponential seismicity model

Zone	Zone name	M_{max}	σM_{max}	M_{min}	M_{max} (obs)	No. of events	β	$\Sigma\beta$	B	σb	λ	σ (λ)	A
	All Aden	**6.8**	**0.3**	**4**	**6.8**	**412**	**1.53**	**0.06**	**0.66**	**0.03**	**11.37**	**0.92**	**3.7**
1	Western Aden	6.9	0.32	4	6.8	165	1.74	0.08	0.76	0.03	4.266	0.315	3.67
2	Alula Fartaq	6.7	0.38	4	6.5	89	1.75	0.09	0.76	0.04	2.344	0.331	3.42
3	Eastern Aden	6.5	0.23	4	6	143	1.64	0.08	0.71	0.04	3.793	0.345	3.42
4	NE Aden	5.8	0.3	4	5.8	15	1.53	0.06	0.66	0.026	0.912	0.053	2.6
5	Yemen	6.6	0.33	4	6.4	25	2.05	0.11	0.89	0.05	0.389	0.099	3.15
	All Owen	**7.0**	**0.34**	**4**	**6.7**	**112**	**1.77**	**0.08**	**0.77**	**0.04**	**3.61**	**0.352**	**3.64**
6	Owen	6.9	0.36	4	6.7	96	1.7	0.09	0.74	0.04	2.512	0.262	3.36
7	Murray	6.4	0.68	4	5.8	16	1.77	0.08	0.77	0.03	0.741	0.073	2.95
8	Oman Mnt.	6.0**	0.5	4	5.5	7	1.83	0.25	0.79	0.11	0.06	0.032	1.95
	All Makran	**8.2**	**0.23**	**4**	**8.1**	**98**	**1.77**	**0.08**	**0.77**	**0.04**	**4.17**	**0.34**	**3.7**
9	East Makran	8.2	0.21	4	8.1	67	1.84	0.09	0.79	0.04	1.862	0.23	3.43
10	West Makran	7.8	0.23	4	7.7	31	2.13	0.11	0.92	0.05	1.04	0.019	3.7
11	Jaz Murian	7.1	0.31	4	7	24	1.81	0.11	0.78	0.05	0.9	0.019	3.07
12	Gowk fault	7.8*	0.52	4	7.1	55	1.89	0.09	0.82	0.04	1.7	0.23	3.51
13	Jiroft-Sabzevaran fault	6.8*	0.25	4	5.8	35	1.94	0.1	0.84	0.04	1.103	0.172	3.4
14	Minab-Zendan	6.7*	0.31	4	5.8	12	1.38	0.13	0.60	0.06	0.44	0.15	2.04
15	Aliabad	7.1	0.52	4	6.6	63	1.9	0.1	0.83	0.04	2.19	0.28	3.66
	All Zagros	**7.2**	**0.17**	**4**	**7.1**	**897**	**1.98**	**0.05**	**0.86**	**0.02**	**25.505**	**0.87**	**4.85**
16	High Zagros Thrust	6.8	0.3	4	6.7	120	1.63	0.08	0.71	0.04	3.298	0.315	3.36
17	Zagros Foredeep	6.9	0.31	4	6.8	156	1.73	0.08	0.75	0.04	4.158	0.217	3.62
18	Arabian Gulf	6.1	0.14	4	6.0	52	1.89	0.1	0.82	0.04	1.474	0.207	3.45
19	Zagros simple fold	7.2	0.31	4	7.1	298	1.97	0.07	0.86	0.03	9.393	0.517	4.41
	Zagros strike-slip Faults	**6.3**	**0.36**	**4**	**6.1**	**54**	**2.12**	**0.1**	**0.92**	**0.04**	**1.772**	**0.242**	**3.92**
20	Borazjan fault	6.8*	0.42	4	5.5	26	2.2	0.13	0.96	0.06	1.010	0.2	3.84
21	Kaserun fault	6.5*	0.57	4	5.9	14	2.11	0.1	0.91	0.04	0.588	0.145	3.43

Table 3 continued

Zone	Zone name	M_{max}	σM_{max}	M_{min}	M_{max} (obs)	No. of events	β	$\Sigma\beta$	B	σb	λ	$\sigma(\lambda)$	A
22	Karebas Fault	6.5*	0.32	4	4.6	8	2.12	0.13	0.92	0.06	0.331	0.114	3.2
23	Sabz Pushan fault	6.4*	0.41	4	6.1	6	2.12	0.1	0.92	0.04	1.047	0.177	3.7
24	Dezful Embayment	6.0	0.34	4	5.8	217	1.71	0.08	0.74	0.04	5.026	0.438	3.66
25	Iranian background	6.7	0.27	4	6.7	39	1.99	0.11	0.86	0.05	1.15	0.215	3.5
26	Arabian background	5.7**	0.5	4	5.2	27	2.22	0.13	0.96	0.06	0.571	0.062	3.6

* Maximum magnitude is calculated using the empirical relationships of Wells and Coppersmith (1994)

** Maximum observed magnitude plus 0.5

When not specified, maximum magnitude is calculated using Kijko (2004)

Bold black fonts are the regional earthquakes recurrence parameters for All Aden, All Owen, All Zagros, and the Zagros strike-slip faults

equation is valid for any cumulative density function (CDF), $F_m(m)$, and does not require the fulfilment of any additional conditions. It may also be used when the exact number of earthquakes, n, is not known. In this case, the number of earthquakes can be replaced by λT. Such a replacement is equivalent to the assumption that the number of earthquakes occurring in unit time conforms to a Poisson distribution with parameter λ, with T the span of the seismic catalogue. It is also important to note that since the value of the integral Δ is never negative, the equation provides a value of $M_{\max}$, which is never less than the largest magnitude already observed. The integration Δ for the Gutenberg-Richter relation that bounded from above is given by:

$$\Delta = \int_{M_{\min}}^{M_{\max}} \left[\frac{1 - \exp[-\beta(m - M_{\min}]}{1 - \exp\left[-\beta(M_{\max}^{\text{obs}} - M_{\min})\right]} \right]^n \mathrm{d}m \tag{4}$$

This integral is not simple to evaluate; therefore, Kijko (2004) replaced $[FM(m)]^n$ by its Cramer (1961) approximation $\exp\{-n[1 - [FM(m)]\}$. Then, the integral is solved to result in $M_{\max}$.

It is also clear that the maximum magnitude of Makran zone obtained using Kijko (2004) approach (Table 3) is less than that found by the characteristic model (Aldama et al. 2009), which is used in the current calculations (Table 2). In Oman Mountains and the Arabian background seismic sources, the maximum magnitude was obtained by adding 0.5 units to the maximum observed magnitude (Table 3).

3.4 Ground-motion prediction equations

The scarcity and lack of ground-motion acceleration records in the Sultanate of Oman makes it a must to apply already developed ground-motion scaling relationships.

Table 4 Characteristics of the ground-motion scaling relationships

Model	Mag.	$M_{\min}$	$M_{\max}$	Dist.	$D_{\max}$	Horizontal comp.	Faulting mechanism	Tectonic
Ambraseys et al. (1996)	M_S	4.0	7.5	R_{JB}	200	Larger horizontal	Unspecified	Shallow active
Boore et al. (1997)	M_W	5.5	7.5	R_{JB}	80	Random horizontal	S.S/Reverse Others	Shallow active
Abrahamson and Silva (Abrahamson and Silva 1997)	M_W	4.4	7.4	R_{rup}	220	Geometric mean	Reverse/ reverse-oblique/ others	Shallow active
Youngs et al. (1997)	M_W	5.0	8.2	R_{rup}	500	Geometric mean	Interface/In-slab	Subduction zones
Atkinson and Boore (2003)	M_W	5.0	8.3	R_{rup}	550	Random horizontal	Interface/In-slab	Subduction zones
Atkinson and Boore (2006)	M_W	3.5	8.0	R_{rup}	1,000	Unspecified	Unspecified	Stable regions

R_{rup} is the minimum distance between the rupture and the site

$M_{\min}$ and $M_{\max}$ are the minimum and maximum magnitude in the model data set

S.S is strike-slip faulting

$D_{\max}$ is the maximum distance in the data set

Alternative ground-motion prediction relationships are selected to predict the seismic hazard within the various considered tectonic environments in order to account for the epistemic uncertainty. This, in turn, implicates several different estimates of the ground motion. Six different ground-motion prediction relationships are selected. These relationships have been widely used in the seismic hazard assessment all over the world.

We used the models of Ambraseys et al. (1996), Abrahamson and Silva (1997) and Boore et al. (1997) to model the ground motions of the earthquakes occurring within the active shallow crustal seismogenic zones. The models of Youngs et al. (1997) and Atkinson and Boore (2003) are used to model the ground motions of Makran subduction zone earthquakes. For the Arabian stable craton earthquakes, the model of Atkinson and Boore (2006) with stress drop 140 bar is used. The definition of the Arabian Peninsula as stable craton is not unambiguously confirmed (Aldama et al. 2009). Thus, the three ground-motion scaling relationships of the active shallow seismicity were used in conjunction with Atkinson and Boore (2006) relationships to model the stable craton ground motion although in a lower weight. The characteristics of the selected ground-motion prediction relationships are shown in Table 4. For the active regions like Zagros, the equation of Ambraseys et al. (1996) is derived from data sets of European and Middle Eastern strong-motion data that include records from Iran. There is increasing evidence that motions in Western North America (WNA), where the data of Boore et al. (1997) were taken, are broadly similar to those from this region (e.g. Stafford et al. 2008).

Combining two or more ground-motion prediction relationships within hazard calculations requires several conversions to be made, because there are several definitions available for both the predicted ground-motion parameters and the explanatory parameters within the ground-motion prediction relationships. Therefore, alternative inputs and outputs must be transformed into a common metrics (Bommer et al. 2005). All of the models used are expressed in terms of moment magnitude except Ambraseys et al. (1996) (See Table 4). Thus, Ambraseys and Free (1997) relationship was used to transform the ground-motion prediction relationships into the moment magnitude scale. In the current PSHA study, distance metrics are handled using the software package of CRISIS 2007, which accepts different definitions of the source to the site distance.

Ground-motion prediction equations have employed a variety of definitions for the horizontal component of motion based on different treatments of the two horizontal traces from each accelerogram. When equations using different horizontal component definitions are combined in a logic tree framework for seismic hazard analysis, adjustments need to be made to both the median values of the predicted ground-motion parameter and to the associated aleatory variability to achieve compatibility among the equations. Ground-motion scaling relations for which the horizontal component is not defined as geometric mean of the two horizontal components are adjusted into this definition using the relationships of Beyer and Bommer (2006) and then introduced into CRISIS 2007.

4 Hazard calculations

The alternative seismic source zonations, alternative activity rates and ground-motion model that have previously been discussed are all incorporated into the hazard calculations through the use of the logic tree formulation. The branched of each stage of the decision-making process with weights as the probability of each are drawn to represent the different options considered. The weights for each stage should sum to unity. Thus, different alternatives for the above input parameters were taken, which in turn implicate several

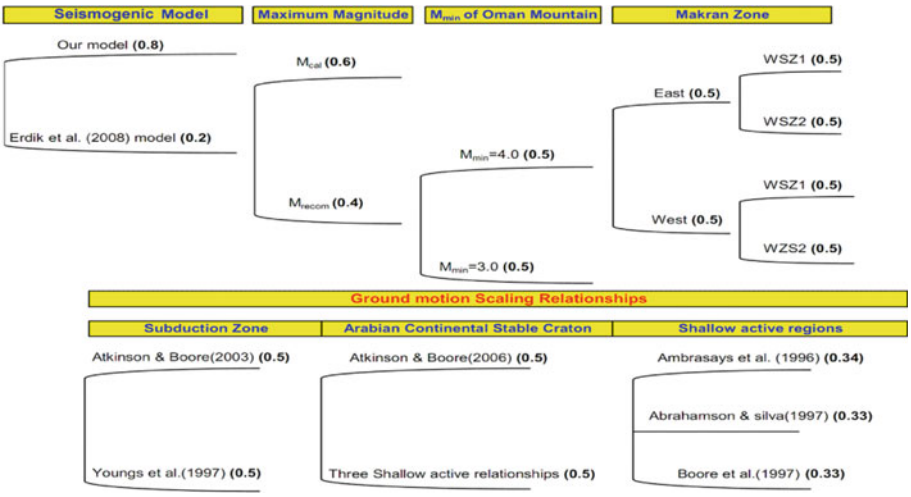

Fig. 11 Components of the logic tree used for hazard calculations, bold numbers are the weights and WSZ1 and WSZ2 are the two likely widths considered for Makran subduction zone

different estimates of the ground motion. Mean and percentile values of the strong-motion parameter obtained from several alternatives could then be calculated.

In the current study, the alternative parameters and their assigned weights are shown in Figure (11). There are four components of the tree that relate to the source zonation and recurrence parameters (upper half of Fig. 11) and one components that relates to the ground-motion models (lower half of Fig. 11). In all cases, the weights have been assigned to the branches through deep discussion among the current authors to reflect their relative confidence in each option.

For the uncertainty associated with the seismotectonic source models, the Erdik et al. (2008) model reflects the regional tectonic setting is given 0.2 weight in the logic tree branch because it lacks the detailed definition of individual faulting structures and it contains no clear background zones to model the floating earthquakes. The developed seismotectonic source model is given 0.8 weight.

The selected minimum magnitude used for calculating the doubly bounded exponential model parameters and calculation of seismic hazard in all seismic zones is 4.0. Oman and Dubai seismic networks provide a complete earthquake catalogue down to magnitude 3.0 in Oman Mountains since 2002. This allows the opportunity to create a new branch on the logic tree for which the minimum magnitude used for calculating the doubly bounded exponential model parameters is selected to be 3.0. The two branches of the minimum magnitude of Oman Mountains have been allocated similar weight, 0.5 for each. The β and λ values are changed slightly from those in Table 3 and both of them are listed below in Table 5. The change in results due to utilizing this new minimum magnitude will be discussed later in this study.

Table 5 Comparison of Oman Mountains' recurrence parameters due to $M_{\min}$ change

Minimum magnitude	b value	σ (b)	a value
3.0	0.78	0.1	2.10
4.0	0.79	0.11	1.95

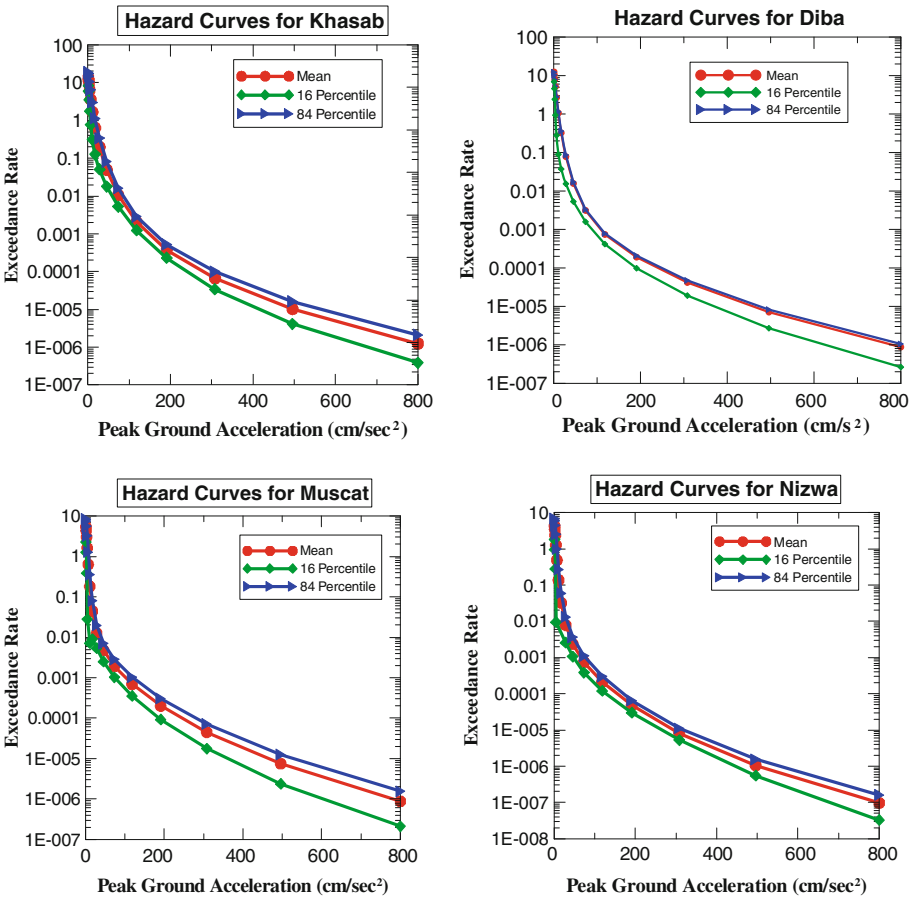

Fig. 12 Seismic hazard curves for four selected sites in Oman

It is important to note in Table 3 that the difference between the maximum observed and the maximum calculated magnitude using Kijko (2004) approach in some seismogenic zones is quite small (e.g. Makran; Jaz Murian, High Zagros; Zagros simple fold … etc.). This motivated the seismic hazard team to suggest creating a new branch on the logic tree by adding an increment (0.2 magnitude units) to these calculated values with very small differences ($\leq$0.2 magnitude units) from the observed ones. The weight given for this recommended maximum magnitude (M_{Recom}) branch is 0.4 because it depends highly on the experts' judgment. The branch of the calculated maximum magnitudes (M_{cal}) is given a weight of 0.6.

Aldama et al. (2009) added the width of the seismogenic zones of Makran subduction zone as a source of uncertainty to be incorporated into logic tree. In the current study, equal weights are given to both assumptions of the width of the seismogenic zones (WSZ1 and WSZ2).

For the ground-motion models in the stable craton, the model of Atkinson and Boore (2006) is favored with a weight of 0.50 being allocated to this model and 0.50 spread

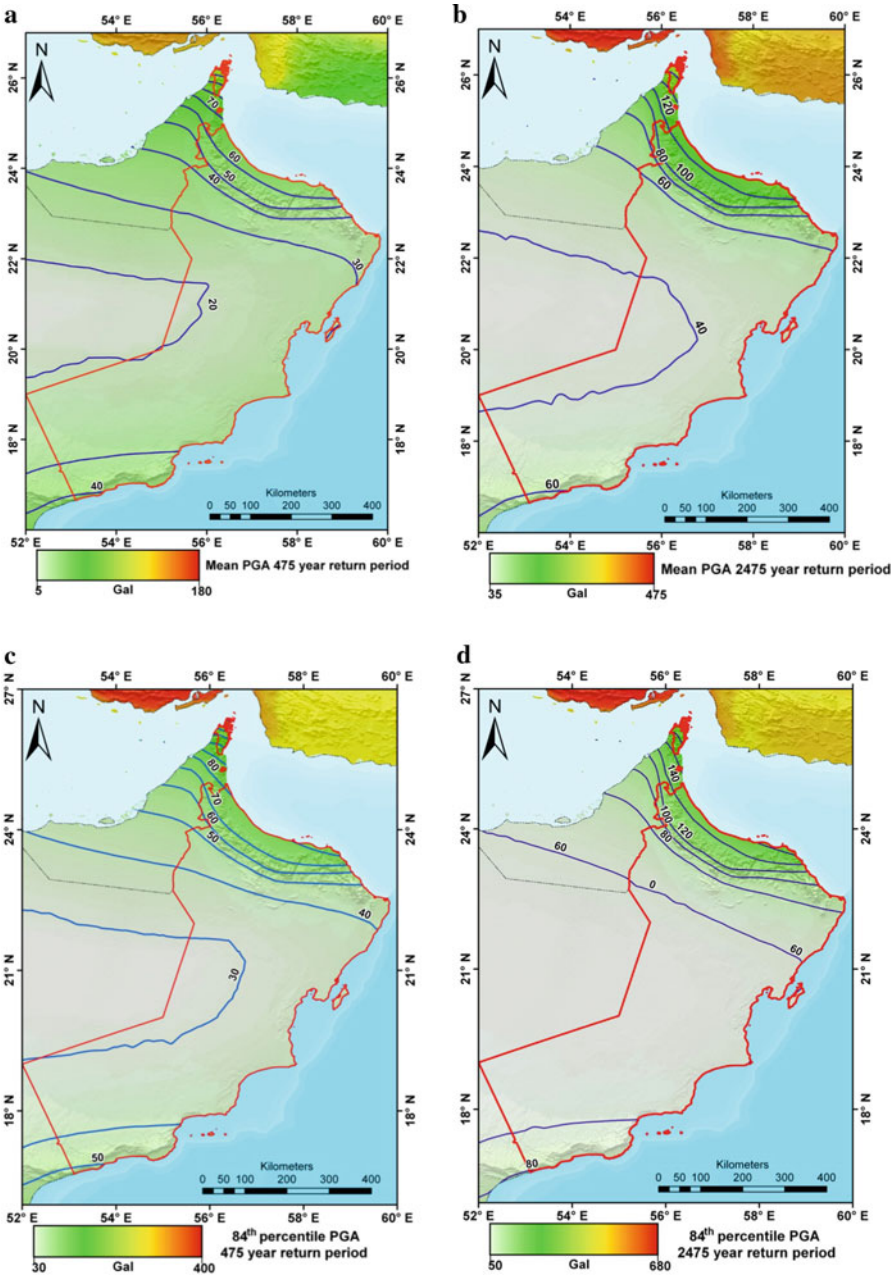

Fig. 13 Mean (**a** and **b**) and 84 percentile (**c** and **d**) peak ground acceleration (cm/s^2) on rock sites with 10 and 2 % probability of being exceeded in 50 years (475 and 2,475 years return periods) in the Sultanate of Oman

equally among the remaining three active shallow models. The subduction zone model of Atkinson and Boore (2003) is given the same weight 0.5 as that of Youngs et al. (1997) model.

5 Results

Selected results only are presented herein; the complete PSHA results for a range of frequencies and return periods, including also uniform hazard spectra, are available in (El-Hussain et al. 2010). First of all, we plotted seismic hazard curves (exceedance rate as a function of peak ground acceleration ranging from 1 to 800 cm/s^2) for four selected cities namely Khasab, Diba, Muscat, and Nizwa in Oman, (Fig. 12). Generally, the hazard level increases toward northeast owing to the increasing proximity of the Zagros and Makran seismogenic zones where relatively higher seismic activity takes place. The hazard is relatively high near Khasab. Diba is situated about 60 km to the south from Khasab; thus, Zagros and Makran seismogenic zones in addition to the local seismicity in Oman Mountains seismogenic zone combine to produce a relatively significant seismic hazard in this city.

Seismic hazard values are calculated over a 0.2° × 0.2° grid extending all over the Sultanate of Oman and its surroundings, for a total number of 2,296 computation nodes. Results from the logic tree are treated to obtain the mean value of the acceleration and values of 84 % percentile at each point. The PGA and 5 % damped horizontal spectral acceleration values at 0.1, 0.2, 0.3, 1.0, 2.0 s spectral periods were mapped so that can be used to generate approximate UHS for each node on the hazard maps for the range of periods important for common engineered structures.

The hazard maps in Fig. (13) display the regional distribution of the mean and 84 percentile PGA in cm/s^2 for a rock condition, with 10 %, and 2 % chance of exceedance in 50 years, which correspond to return periods of 475 and 2,475 years, respectively. The maps delineate the northeastern region of relatively higher seismic hazard from the rest of the country which is characterized by its relatively lower hazard levels. The mean PGA across Oman ranges between 20 and 110 cm/s^2 for 475 years return period and between 40 and 180 cm/s^2 for 2,475 years return period. The highest predicted ground-motion values occur in the extreme north at Khasab City as a result of ground motion from more frequent, larger earthquakes in Zagros seismogenic zones. The relatively moderate hazard of Muscat is due to its proximity to Makran seismogenic zone. Oman Mountains and Arabian background seismogenic zones have a low rate of earthquake activity and result in relatively low ground motion over broad inland areas. The acceleration levels for a 2,475 years return period are around 40 % higher in the northern part of country than those for a 475 years return period. For the western middle region, this increase is up to 100 %.

Figure 14 shows the 5 % damped horizontal spectral acceleration values at 0.1 and 0.2 s spectral period for the two selected return periods. The maximum ground-motion values are associated with the 5 % damped horizontal spectral acceleration with a spectral period of 0.2 s, where the maximum ground motions reach 250, and 400 cm/s^2 for 475 and 2,475 years return periods, respectively, at the most northern part of the country. Computation results clearly indicate that, compared with countries of high seismic risk, seismic hazard in Oman can be described as "low in the southern and western parts to moderate in the northeast".

The plots of the hazard maps of 1 and 2 s spectral periods are normally much lower than the ones for higher frequencies (Fig. 15). In addition, one notices that the high hazard in these maps is slightly less concentrated than those on 0.1 and 0.2 s maps, which is a result of the rapid attenuation of short period ground motion with distance. The consequence is that adjacent sites may have different short period hazard. The steep gradient has negative impact on the engineering design as small changes in the input parameters (e.g. source boundary) can have a large consequence on the hazard at the interested site.

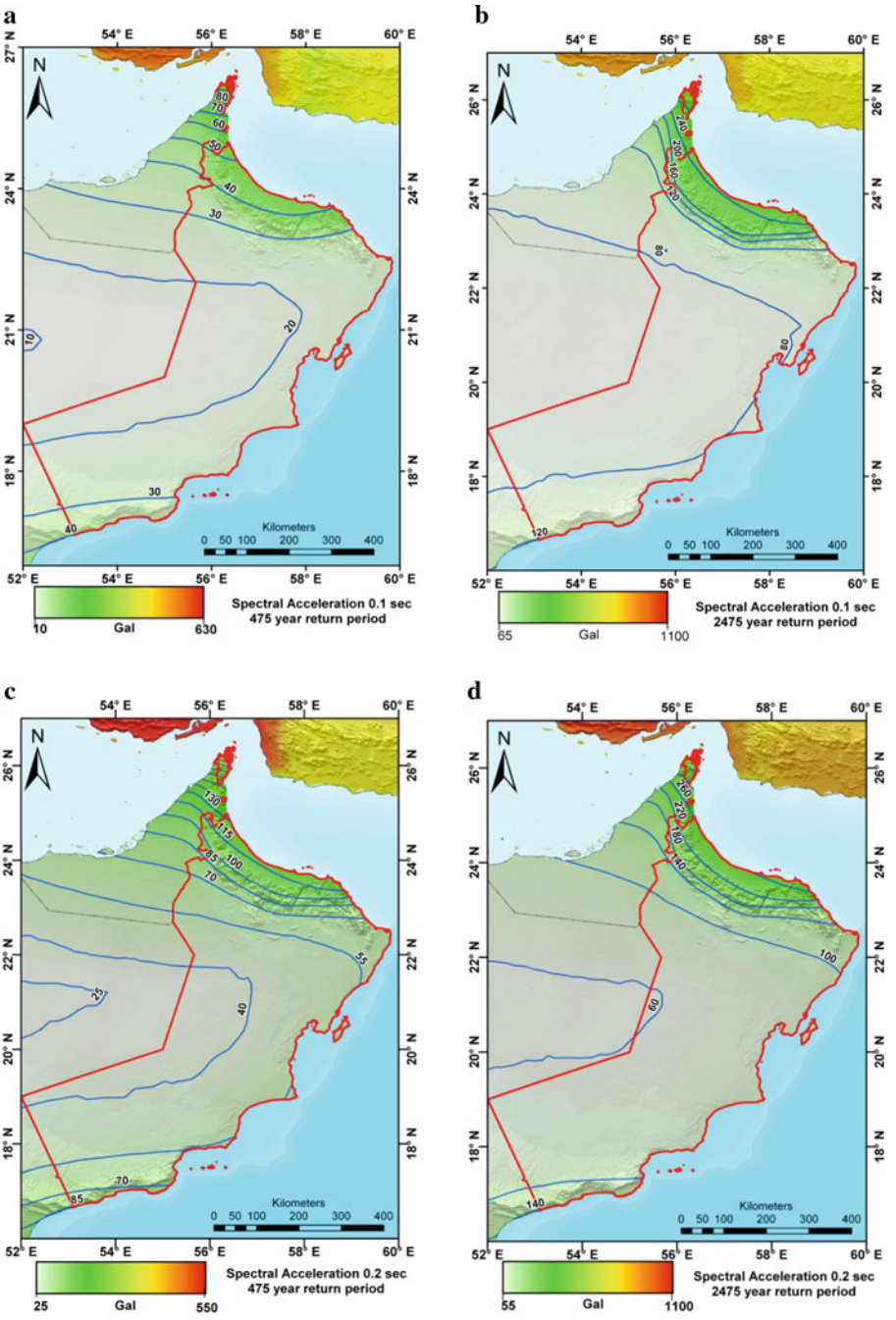

Fig. 14 Mean 0.1 s (**a** and **b**) and 0.2 s (**c** and **d**) spectral acceleration (cm/s^2) on rock sites with 10 and 2 % probability of being exceeded in 50 years (475 and 2,475 years return periods) in the Sultanate of Oman

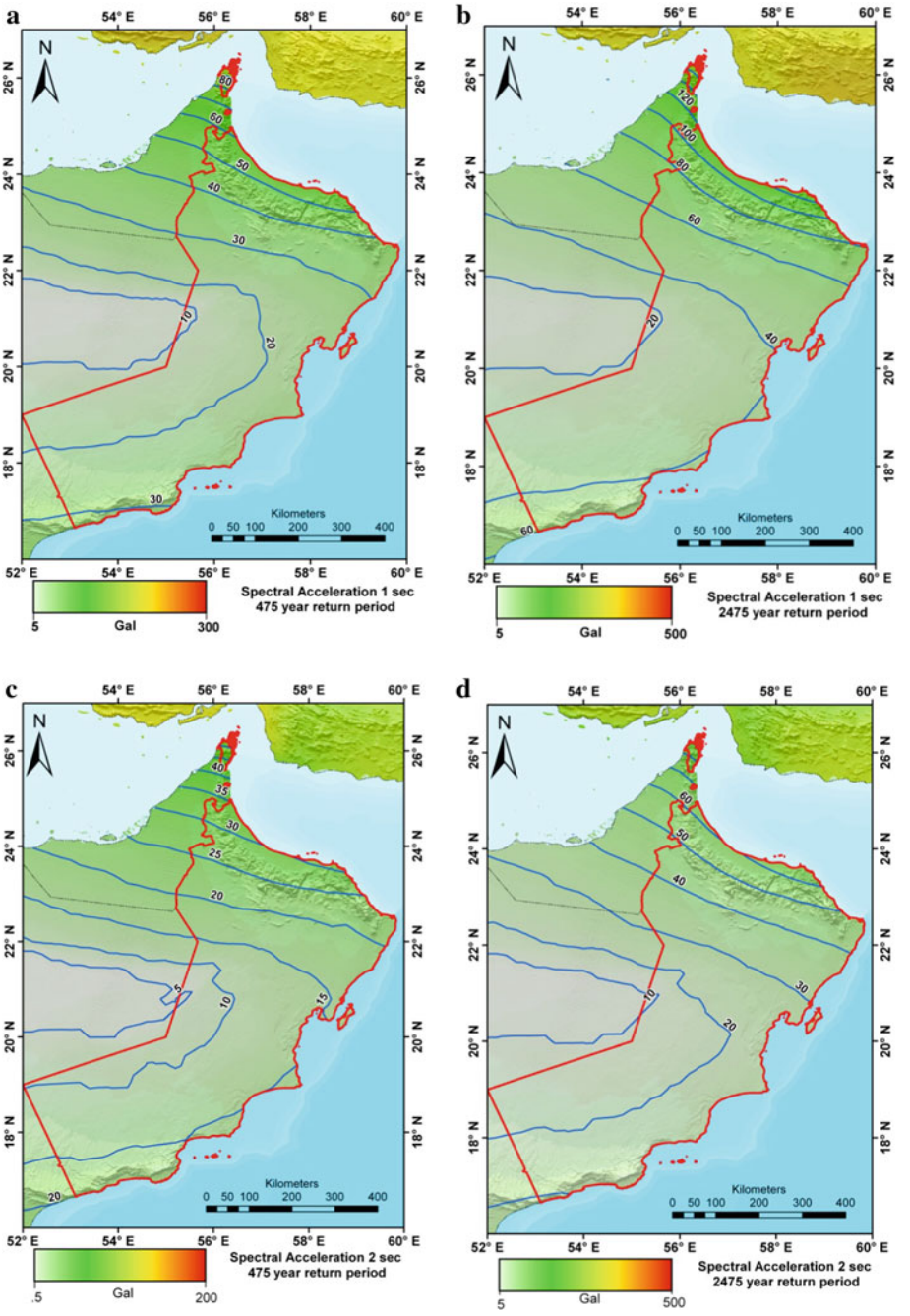

Fig. 15 Mean 1.0 s (**a** and **b**) and 2.0 s (**c** and **d**) spectral acceleration (cm/s^2) on rock sites with 10 and 2 % probability of being exceeded in 50 years (475 and 2,475 years return periods) in the Sultanate of Oman

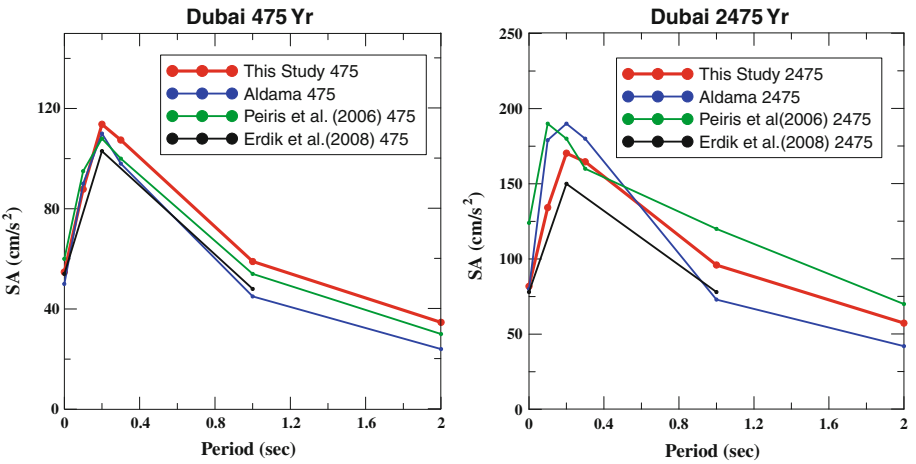

Fig. 16 Uniform hazard spectra for rock sites in Dubai for 475 and 2,475 years return periods from the current study and those of Peiris et al. (2006), Erdik et al. 2008, and Aldama et al. 2009

The geometry of the seismic source zones pattern highly controls the results. This is evident in all maps even the long period ones (2.0 s). The hazard maps thus highly reflect the general tectonic setting of the studied area. The contour maps presented here allow an engineer to construct an approximate UHS for any rock site in Oman.

The results of the current study are extended to Dubai City of UAE in order to compare the results of the current study with those of three recent studies for Dubai (Peiris et al. 2006; Erdik et al. 2008; Aldama et al. 2009). The three studies estimate the seismic hazard at rock sites. As in the current study, Aldama et al. (2009) adjusted their horizontal ground motion of the used ground-motion prediction equations to be identified in terms of geometric mean. Peiris et al. (2006) and Erdik et al. (2008), however, used a number of ground-motion prediction equations that used different distance and horizontal component definitions, and they stated nothing about the adjustments required for the horizontal component compatibility.

Figure 16 shows good agreement among the results of the current study and those of Peiris et al. (2006); Erdik et al. 2008; and Aldama et al. 2009. Comparison with the results of Aldama et al. (2009) shows consistently close agreement at short periods, although the long-period spectral ordinates from Aldama et al. (2009) are generally slightly lower than that of Peiris et al. (2006) and the current study. This difference could be attributed mainly to the use of different ground-motion prediction equations for the shallow seismogenic zones which are the greatest contributor to the seismic hazard at these longer periods (as will be demonstrated in the deaggregation section). Peiris et al. 2006 study shows relatively larger PGA values than the other three studies for 2,475 years return period. The difference between the current study and that of Peiris et al. (2006) and Erdik et al. (2008) could be the result of different definitions of seismogenic zones, ground-motion prediction relationships, and the probable different definitions of the output horizontal ground-motion component. The overlap between the results of this study and others instills further confidence in the Oman results.

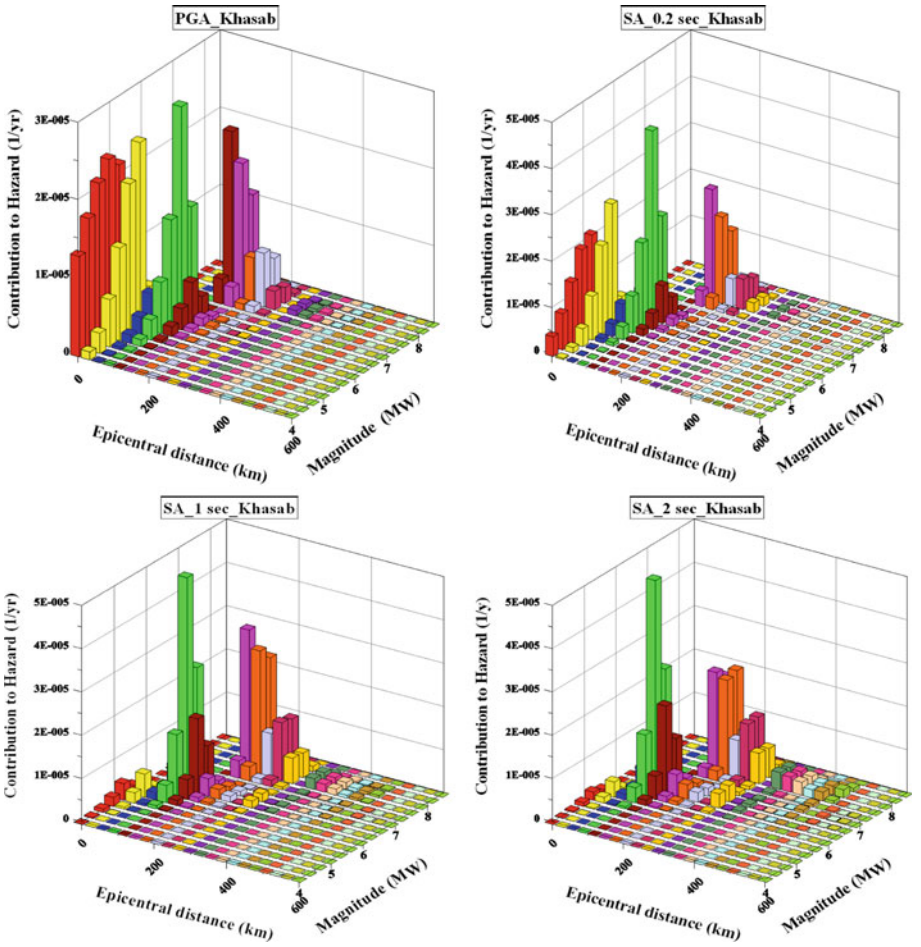

Fig. 17 Deaggregation results showing the relative contribution to the peak ground acceleration and spectral accelerations of 0.2, 1.0, and 2.0 s as a function of magnitude and distance at rock site in Khasab City for return period of 2,475 years

6 Deaggregation of hazard results

The hazard curves were deaggregated to determine the sources that contribute at hazard levels of 10 and 2 % probability of exceedance in 50 years. Following Aldama et al. (2009), the weighted mean of the deaggregation results is adopted like the hazard values. Equal spacing in magnitude and distance is used to express the deaggregation results. We show, for example, results from Khasab and Muscat for 2,475 years return period for 5 % damped spectral acceleration at PGA and spectral periods 0.2, 1.0, and 2.0 s in Figs. 17 and 18. Table 6 shows only the largest contribution to the seismic hazard for 7 cities in Oman for return period 475 years. This table does not reflect the relative contribution of each zone to the assessed hazard. The results of the deaggregation are different for different probability levels and for different spectral periods as indicated by Figs. 17 and 18 and Table 5.

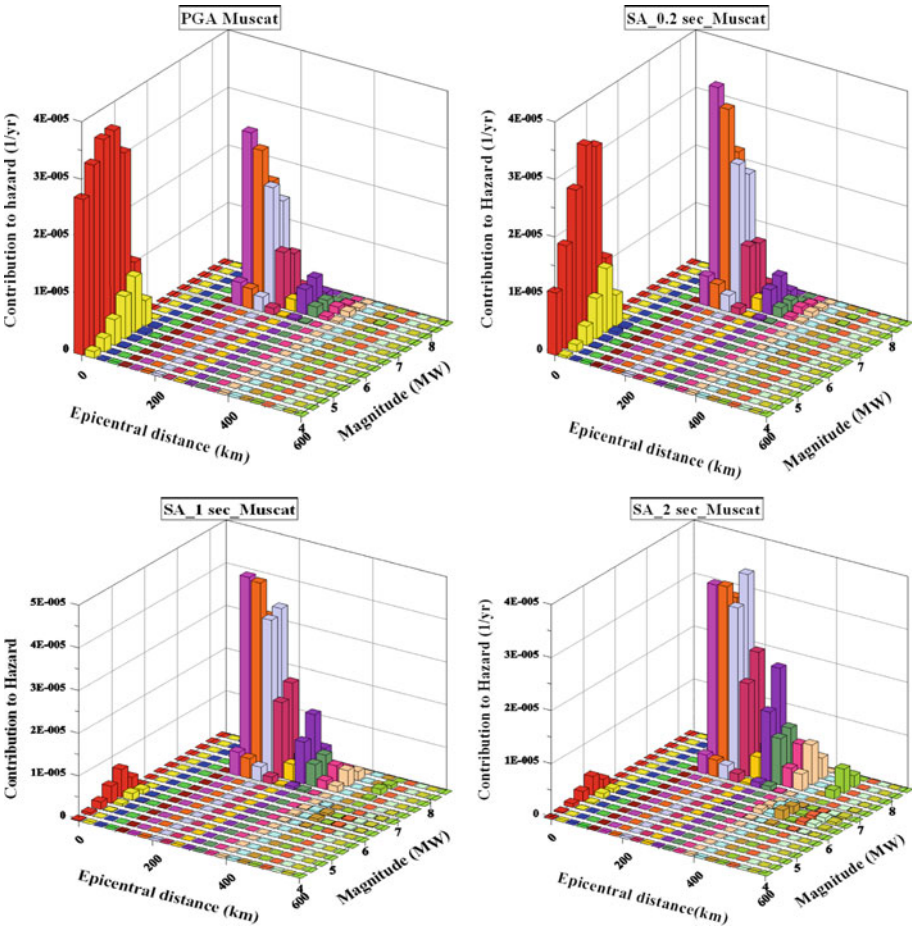

Fig. 18 Deaggregation results showing the relative contribution to the peak ground acceleration and spectral accelerations of 0.2, 1.0, and 2.0 s as a function of magnitude and distance at rock site in Muscat City for return period of 2,475 years

Table 6 Deaggregation of seismic hazard for return periods 475 years

City	PGA 475 year		0.2 s 475 year		1.0 s 475 year		2.0 s 475 year	
	D (km)	M_W	D (km)	M_W	D (km)	M_W	D (km)	M_W
Khasab	90	6.25	90	6.25	90	6.25	90	6.25
Diba	180	7.5	180	7.5	180	7.5	180	7.5
Sohar	240	7.5	240	7.5	240	7.5	240	7.5
Muscat	210	7.5	210	7.5	210	7.5	210	7.5
Nizwa	330	7.5	330	7.5	330	7.5	330	7.5
Sur	300	7.5	390	7.8	390	7.8	390	7.8
Salalah	270	5.6	270	5.9	300	5.9	300	5.9

D is the distance from the seismic source to the site of interest

Earthquakes at a distance of 90 km from Khasab City contribute most to the hazard of this city at both 2 and 10 % levels for all considered spectral periods (Fig. 17 and Table 5). Earthquake with moment magnitude range 6.5–6.75 contributes most to the hazard. This is mainly because the seismicity close to the site of interest is low compared with those at Zagros seismogenic zones. The second most important source for short periods (PGA and 0.2 s) and 2,475 years return period is the Oman Mountains with lower magnitudes. For these short spectral periods, potential large earthquakes of the Makran subduction zone do not contribute as much to the seismic hazard at the Khasab site. However, subduction events may be important at longer spectral periods for consideration in design because of the long duration and less attenuation of the strong ground shaking associated with the possibly generated larger earthquakes.

For Muscat City and for 475 years return period, the hazard is dominated by large distant earthquakes at all response periods (Table 5), while for the 2,475 years return period, the hazard is dominated by nearby small to moderate earthquakes for short spectral periods and by distant larger events for longer ones (Fig. 18). This indicates that seismic sources very close to this city are of low activity rates and high ground-motion levels at short distance are not likely to occur. It is, thus, interesting to note here that for long return periods the rare largest events ($M \geq 7$) are a significant contributor to design hazard. Thus, Zagros and Makran zones have considerable contribution of seismic hazard at Muscat. For

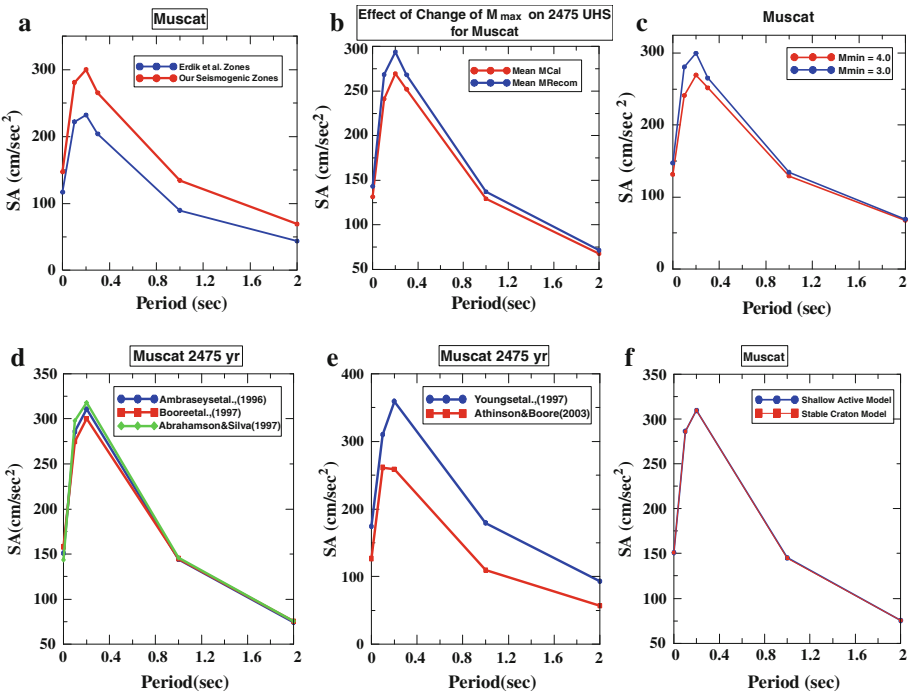

Fig. 19 Five percentage damped acceleration unified hazard spectra in cm/s^2 for a site in Muscat City; each panel evaluates the sensitivity to a specific input parameter of the hazard model: a seismogenic source model; b maximum magnitude; c minimum magnitude at Oman Mountains; d shallow seismic ground-motion prediction models; e subduction ground-motion prediction models; f stable craton ground-motion prediction models

the cities of Sohar, Diba, Nizwa, and Salalah (not shown herein) the situation is similar to that in Muscat.

Although the closer-by distance seismogenic zones of Oman Mountains and the closer Arabian craton have the largest contribution on the short spectral period seismic hazard for 2,475 years return period at most cities (Khasab is exceptions), moderate magnitude (4.5–5.0) is responsible for such contribution (Fig. 18). Contribution of earthquakes with larger magnitudes from Oman Mountains and the Arabian stable craton needs longer return period.

7 Sensitivity analysis

Sensitivity analysis is conducted in order to detect which parameters are the most critical for the hazard computation. The purpose of the current sensitivity analysis is to see how the variations in the alternative parameter assessments influence PSHA statistics. The findings of the sensitivity analysis are used to focus efforts on refining the PSHA results.

Figure 19-a shows sensitivity analysis for six parameters represented as uniform hazard spectra computed for 2,475 years return period and rock sites in the Muscat city as an example. The sensitivity analysis assisted in determining the effect of the change of the seismotectonic source model (our developed model or Erdik et al. 2008 model) on the resultant ground motion. At Muscat, where the Makran subduction zone has a considerable contribution to seismic hazard, the hazard resulting from using our model is about 20 % higher than that of Erdik et al. (2008). This could be mostly attributed to the higher maximum magnitude used in our model for Makran zones and partially due to the different treatment of the seismicity parameters in the two models (characteristic and doubly bounded exponential model).

The choice of the maximum magnitude has a minor influence on the hazard at Muscat City (Fig. 19b). This minimal change is due to the remoteness of the seismogenic zones for which the maximum magnitude is changed (Table 3). The choice of the minimum magnitude to calculate the exponential double bound model parameters of Oman Mountains' seismogenic zone has a moderate influence on the final hazard at Muscat. Figure 19c shows that the change from 4.0 to 3.0 minimum magnitude increases the seismic hazard of Muscat City by about 12 % at 0.1 and 0.2 s spectral periods.

As a demonstration of the sensitivity of the results due to the choice of the shallow active ground-motion prediction equations, a series of hazard UHS is presented for the Muscat City. Figure 19d compares the results obtained from Ambraseys et al. (1996), Boore et al. (1997), and Abrahamson and Silva (1997), which are employed in the current study. The three models selected for this study are in rather good agreement at Muscat City. The results based on Abrahamson and Silva (1997) seem to be the outlier for the short spectral periods. Figure 19e compares the effect of changing the ground-motion scaling relationships of the subduction zone earthquakes, with the UHS based upon Youngs et al. (1997) being up to one-third higher than those resulted from Atkinson and Boore (2003). The ground-motion prediction equations of the subduction zone earthquakes influence the hazard results quite strongly. This may be explained by the fact that the contribution to the hazard from the subduction zones is dominated by large events of relatively large distance where the difference between the two ground-motion scaling relationships is largest.

The sensitivity analysis of the ground-motion scaling of the Arabian stable craton is done by comparing the results based upon Atkinson and Boore (2006) model with the mean results of Ambraseys et al. (1996), Boore et al. (1997), and Abrahamson and Silva

(1997). Due to the low seismicity of the stable craton back ground seismogenic zone, the change of the ground-motion scaling relationships has no effect at all at Muscat, which is relatively remote from this seismogenic zone (Fig. 19f).

8 Discussion

The seismic hazard assessment in Oman presented in the current study was developed with the consideration of the limited database and scientific knowledge regarding the seismogenic nature of the region, particularly Oman Mountains. The hazard maps are submitted herein to define the seismic hazard as reasonably as possible using existing data and information. Three fruitful areas of further study can be recommended: (1) historical and contemporary earthquake studies, (2) studies in contemporary tectonics and paleoseismicity in Oman, and (3) developing regional ground-motion scaling relationships for Oman.

In terms of instrumental seismicity, most of Oman appears as aseismic. The historical accounts of strong shaking at Qalhat, Nizwa, and Sohar are indications that a potentially serious seismic hazard may exist in Oman. Geological field investigations of the reported disruptions in these areas could serve to confirm or deny the historical reports.

It is very important in seismic fault studies of Oman Mountains to distinguish paleoseismic tectonic fault rupture from faulting due to any other reason (regional uplifting, flowage, solution, etc.). Hazard estimates can change dramatically for specific areas when causal seismogenic faults are identified and the earthquake occurrence frequencies and maximum magnitudes are determined specifically for such faults. The consequence is that the hazard can be tied to specific faults rather than averaged over broad areas, thus resulting in a more accurate portrayal of a more local seismic hazard.

The probabilistic seismic hazard maps deal with ground motion on rock; thus, the current analysis did not consider the amplification of soils or basins responses. These factors can change the ground motions and should be considered in the analysis of any site with ground conditions different from rock.

However, the used ground-motion prediction equations can be tested and refined by installing an accelerographic system for continuous recording within the Oman territory. Refining or even developing new ground-motion prediction equations for our specific region would ultimately lead to a better estimate of seismic hazard.

9 Conclusions

This current study provides national seismic hazard maps for the purposes of seismic zoning and developing of Oman seismic building code. Maps are provided, with return periods of 475 and 2,475 years, showing horizontal peak ground acceleration (PGA), and 0.1, 0.2, 0.3, 1.0, and 2.0 s spectral accelerations for rock site conditions. Uncertainties in seismic sources, maximum magnitude, and ground-motion models have been incorporated in the seismic hazard model using a logic tree framework. The results conclude that the seismic hazard in most of Oman is low and for normal engineering structures, seismic design may not be required, except in the most northeastern area of the country. The deaggregation of seismic hazard results demonstrates that distant seismogenic sources have the greatest contribution for most sites for all spectral periods at 475 years return period while for the 2,475 years return period, the hazard is dominated by nearby small to moderate earthquakes for short spectral periods and by distant larger events for longer

ones. The sensitivity analysis for the results at Muscat City proves that the biggest uncertainties in the current analysis probably stem from the choice of the seismogenic model and the subduction ground-motion prediction relations. Therefore, refinement of the ground-motion prediction relations in the study area is crucial.

It is not considered the best practice to only use values on the maps as design coefficients replacing site-specific studies for important structures. Coupling the current results with the site-specific characteristics is crucial for these important structures to fully obtain the seismic design coefficients.

Acknowledgments We would like to express our appreciation to the Oman Ministerial Cabinet for funding this project under project number 22409017. Our sincere thanks are also due to Sultan Qaboos University, for the strong support, and encouragement. We would like to express our sincere thanks to Seismic Hazard committee members for their continuous interest and its assistance to complete this work.

References

Abrahamson NA, Bommer JJ (2005) Probability and uncertainty in seismic hazard analysis. Earthq Spectra 21:603–607

Abrahamson NA, Silva WJ (1997) Empirical response spectra attenuation relations for shallow crustal earthquakes. Seismol Res Lett 68:94–127

Al Marzooqi A, Abou Elenean KM, Megahed AS, El-Hussain I, Rodgers AJ, Al Khatibi E (2008) Source parameters of March 10 and September 13, 2007, United Arab Emirates earthquakes. Tectonophys. 460:237–247

Aldama BG, Bommer JJ, Fenton CH, Staford PJ (2009) Probabilistic seismic hazard analysis for rock sites in the cities of Abu Dhbi, Dubai and Ra's Al Khymah, United Arab Emirates. Georisk 3:1–29

Allen CR (1975) Geological criteria for evaluating seismicity. Geol Soc Am Bull 86:1041–1075

Allen M, Jackson JA, Walker R (2004) Late Cenozoic reorganization of the Arabia-Eurasia collision and the comparison of short-term and long-term deformation rates. Tectonics 23, TC2008

Alsinawi SA (1983) Dhamar Earthquake of 13/12/82. A report Submitted to the Yemeni Government, (Arabic text)

Alsinawi SA, Al-Salim MA (1985) The Dhamar Earthquake of 13 December 1982. Proceedings, Second Geol. Congress on the Middle East (Geocome-li) 13:1–139, Baghdad

Ambraseys NN, Bilham R (2003) Earthquakes in Afghanistan. Seismol Res Lett 74:107–123

Ambraseys NN, Free MW (1997) Surface-wave magnitude calibration for European region earthquakes. J Earthq Eng 1:1–22

Ambraseys NN, Melville CP (1982) A history of Persian earthquakes. Cambridge Univ Press, Cambridge

Ambraseys NN, Melville CP, Adams RD (1994) The seismicity of Egypt, Arabia and Red Sea. Cambridge Univ Press, Cambridge

Ambraseys NN, Simpson KA, Bommer JJ (1996) The prediction of horizontal reponse spectra in Europe. Earthq Eng Struct Dyn 25:371–400

ASC (2003) 1945 – Off the Makran Coast (Balochistan), Pakistan, Mw 8.0: Amateur Seismic Center. http://asc-india.org/gq/mekran.htm

Atkinson GM, Boore DM (2003) Empirical ground-motion relations for subduction-zone earthquakes and their application to Cascadia and other regions. Bull Seismol Soc Am 93:1703–1729

Atkinson GM, Boore DM (2006) Earthquake ground-motion prediction equations for Eastern North America. Bull Seismol Soc Am 96:2181–2205

Aubin J (1973) Le Royaume d'Ormuz au de′but du XVIe Sie'cle. Mare Luso-Indicum 4:77–179

Baker C, Jackson J, Priestley K (1993) Earthquakes on the Kazerun line in the Zagros mountains of Iran: strike-slip faulting within a fold-and-thrust belt. Geophys J Int 115:41–61

Bayer R, Chery J, Tatar M, Vernant Ph, Abbassi M, Masson F, Nilforousshan F, Doerflinger E, Regard V, Bellier O (2006) Active deformation in Zagros-Makran transition zone inferred from GPS measurements. Geophys J Int 165:373–381

Bender BK, Perkins DM (1987) SEISRISK III: a computer program for seismic hazard estimation. USGS Open File, Report, pp 82–293

Berberian M (1973) The seismicity of Iran, preliminary map of epicenters and focal depths, 1:2500000 Map Geol. Surv. Seismotectonic Group, Iran

Berberian M (1995) Master 'blind' thrust faults hidden under the Zagros folds, active basement tectonics and surface morphotectonics. Tectonophys 241:193–224
Berberian M, Yeates RS (1999) Patterns of historical earthquake rupture in the Iranian Plateau. Bull Seismol Soc Am 89:120–139
Berberian M, Jackson J, Fielding E, Parsons B, Priestley K, Qorashi M, Talebian M, Walker R, Wright T, Baker C (2001) The 1998 March 14, Fandoqa earthquake (Mw 6.6) in Kerman province, southeast Iran: re-rupture of the 1981 Sirch earthquake fault, triggering of slip on adjacent thrusts and the active tectonics of the Gowk fault zone. Geophys J Int 146:371–398
Beyer K, Bommer JJ (2006) Relationships between median values and between aleatory variablilities for different definitions of the horizontal component of motion. Bull Seismol Soc Am 96:1512–1522, Erratum (2007) 97:1769
Bommer JJ, Scherbaum F, Bungum H, Cotton F, Sabetta F, Abrahamson NA (2005) On the use of logic trees for ground-motion prediction equations in seismic hazard analysis. Bull Seismol Soc Am 95:377–389
Bonilla MG, Mark RK, Lienkaemper JJ (1984) Statistical relations among earthquake magnitude, surface rupture length, surface rupture displacement. Bull Seismol Soc Am 74:2379–2411
Boore DM, Joyner WB, Fumal TE (1997) Equations for estimating horizontal response spectra and peak acceleration from Western North American earthquakes: a summary of recent work. Seismol Res Lett 68:128–153
Bosworth W, Huchon P, McClay K (2005) The red sea and the Gulf of Aden basins. J Af Earth Sci 43:334–378
Byrne DE, Sykes LR, Davis DM (1992) Great thrust earthquakes and aseismic slip along the plate boundary of the makran subduction Zone. J Geophys Res 97:449–478
Carbon D (1996) Tectonique post-obduction des montagnes d'Oman dans le cadre de la convergence Arabie-Iran. Ph.D. Thesis, University of Montpellier 2, Montpellier, France
Chase CG (1978) Plate kinematics: the American, East Africa, and the rest of the world. Earth Planet Sci Lett 37:355–368
Coppersmith KJ, Youngs RR (1986) Capturing uncertainty in probabilistic seismic hazard assessments within intraplate tectonic environments. In: Proceedings of the Third US national conference on earthquake engineering 1:301–312
Cornell CA (1968) Engineering seismic risk analysis. Bull Seismol Soc Am 18:1583–1606
Cornell CA, Vanmarcke EH (1969) The major influences on seismic risk. In: Proceedings of the fourth world conference of earthquake engineering, 1, Santiago, Chile 69–83
Cramer H (1961) Mathematical methods of statistics, 2nd edn. Princeton University Press, Princeton
Deif A, Abou Elenean K, El-Hadidy M, Tealeb A, Mohamed A (2009) Probabilistic seismic hazard maps for Sinai Peninsula. Egypt J Geophys Eng 6:288–297
DeMets C (2008) Arabia's slow dance with India. Nat Geosci 1:10–11
Dunbar PK, Lockridge PA, Whiteside LS (2002) Catalog of Significant Earthquakes (2150 B.C.–1991 A.D.). National Oceanic and Atmospheric Administration Report SE-49
El-Hussain I, Deif A, Al-Jabry K, Al-Hashmi S, Al-Toubi K, Al-Shijby Y, Al-Saify M (2010) Probabilistic and deterministic seismic hazard assessment for Sultanate of Oman (Phase I). Project #22409017, submitted to Sultan Qaboos Univeristy, Oman
Engdahl ER, Van Der Hilst R, Buland R (1998) Global teleseismic earthquake relocation with improved travel times and procedures for depth determination. Bull Seismol Soc Am 88:722–743
Erdik M, Demircioglu B, Sesetyan K, Durukal E (2008) Probabilistic seismic hazard assessment for Dubai. Boğaziçi University, Kandilli Observatory and Earthquake Research Institute Department of Earthquake Engineering
Farhoudi G, Karig DE (1977) Makran of Iran and Pakistan as an active arc system. Geol. 5:664–668
Fenton CH, Adams J, Halchuk S (2006) Seismic hazards assessment for radioactive waste disposal sites in regions of low seismic activity. Geotech Geol Eng 24:579–592
Fournier M, Chamot-Rooke N, Petit C, Fabbri O, Huchon P, Maillot B, Lepvrier C (2008) In situ evidence for dextral active motion at the Arabia-India plate boundary. Nat Geosci 1:54–58
Frankel A (1995) Mapping seismic hazard in the central and eastern United States. Seismol Res Lett 66:8–21
Frankel A, Mueller C, Barnhard T (1997) Seismic hazard maps for California. Nevada and western Arizona/Utah. United States Geological Survey, Open-File Report, pp 97–130
Gardner JK, Knopoff L (1974) Is the sequence of earthquakes in Southern California, with aftershocks removed, Poissonian? Bull Seismol Soc Am 64:1363–1367
Gholamzadeh A, Yamini-Fard F, Hessami K, Tatar M (2009) The February 28, 2006 Tiab earthquake, Mw 6.0: implications for tectonics of the transition between the Zagros continental collision and the Makran subduction zone. J Geodyn 47:280–287

Giardini D, Grünthal G, Shedlock KM, Zhang PZ (1999) The GSHAP global seismic hazard map. Ann Geofis 42:1225–1230
Gillard D, Wyss M (1995) Comparison of strain and stress tensor orientation: application to Iran and southern California. J Geophys Res 100:22197–22213
Grunthal G, Wahlstrom R (2003) An Mw based earthquake catalogue for central, northern and northwestern Europe using a hierarchy of magnitude conversions. J. Seismol. 7:507–531
Gutenberg B, Richter CF (1944) Frequency of earthquakes in California. Bull Seismol Soc Am 34:185–188
Hanks TC, Bakun WH (2002) A bilinear source-scaling model for M-log (A) observations of continental earthquakes. Bull Seismol Soc Am 92:1841–1846
Hatzfeld D, Authemayou C, Van der Beek P, Bellier O, Lave J, Oveisi B, Tatar M, Tavakoli F, Walpersdorf A, YaminikFard F (2010) The kinematics of the Zagros Mountains (Iran). In: Tectonic and Stratigraphic Evolution of Zagros and Makran During the MesozoickCenozoic, edited by P. Leturmy and C. Robin, Geol. Soc. Spec. Publ. 330:19–42
Hessami K, Koyi H, Talbot C (2001) The significance of the strike-slip faulting in the basement of the Zagros fold and thrust belt. J Petrol Geol 24:5–28
Hessami K, Jamali F, Tabassi H (2003) Major active faults in Iran. Ministry of Science, Research and Technology, International Institute of Earthquake Engineering and Seismol. (IIEES), 1:250000 scale map
Hessami K, Nilforoushan F, Talbot C (2006) Active deformation within the Zagros Mountains deduced from GPS measurements. J Geol Soc 163:143–148
Jackson JA, Fitch T (1981) Basement faulting and the focal depths of the larger earthquakes in the Zagros Mountains (Iran). Geophys J R Astron Soc 64:561–586
Jackson JA, McKenzie D (1984) Active tectonics of the Alpine-Himalayan Belt between western Turkey and Pakistan. Geophys J R Astron Soc 77:185–264
Johnson PR (1998) Tectonic map of Saudi Arabia and adjacent areas. Deputy Ministry for Mineral Resources, USGS TR-98-3, Saudi Arabia
Johnson AC, Coppersmith KJ, Kanter LR, Cornell CA (1994) The earthquakes of stable continental regions. In: Schneider JF (ed) Assessment of large earthquake potential, 1. Electric Power Research Institute, Palo Alto
Kijko A (2004) Estimation of the maximum earthquake magnitude. Mmax Pure Appl Geophys 161:1655–1681
Kopp C, Fruehn J, Flueh ER, Reichert C, Kukowski N, Bialas J, Klaeschen D (2000) Structure of the Makran subduction zone from wide angle and reflection seismic data. Tectonophys 329:171–191
Kukowski N, Schillhorn T, Flueh ER, Huhn K (2000) Newly identified strike-slip plate boundary in the northeastern Arabian Sea. Geol 28:355–358
Kusky T, Robinson C, El-Baz F (2005) Tertiary-Quaternary faulting and uplift in the northern Oman Hajar Mountains. J Geol Soc 162:871–888
Langer CJ, Bollinger GA, Merghelani HM (1987) Aftershocks of the 13 December 1982 North Yemen earthquakes: conjugate Normal Faulting in an extensional setting. Bull Seismol Soc Am 77:2038–2055
Maggi A, Priestley K, Jackson J (2002) Focal depths of moderate and large size earthquakes in Iran. J Seismol Earthq Eng 4:1–10
McGuire RK (1976) FORTRAN computer programs for seismic risk analysis. US Geol. Survey Open-File Report No 76-67
McGuire RK (1978) FRISK: Computer program for seismic risk analysis using faults as earthquake sources. US Geological Survey Open-File Rep. pp 78–107
McKenzie DP, Sclater JG (1971) The evolution of the Indian ocean since the Late Cretaceous. Geophys J R Astron Soc 24:437–528
Minster JB, Jordan TH (1978) Present-day plate-motion. J Geophys Res 83:5331–5354
Minster JB, Jordan TH, Molnar P, Haines E (1974) Numerical modeling of instantaneous plate tectonic. Geophys J R Astron Soc 36:541–576
Musson RMW (2009) Subduction in the Western Makran: the historian's contribution. J Geol Soc Lond 166:387–391
Ni J, Barzangi M (1986) Seismotectonics of the Zagros continental collision zone and a comparison with the Himalayas. J Geophys Res 9:8205–8218
Nowroozi N (1972) Focal mechanism of earthquakes in Iran, Turkey, West Pakistan and Afghanistan and plate tectonics of the Middle East. Bull Seismol Soc Am 62:823–850
Ordaz M, Aguilar A, Arboleda J (2007) CRISIS 2007. Institute of Engineering, UNAM, Mexico-City, Mexico

Pararas-Carayannis G (2004) Seismo-dynamics of compressional tectonic collision-potential for tsunami genesis along boundaries of the Indian, Eurasian and Arabian plates. Abstract submitted to the International Conference HAZARDS 2004, Hyderabad, India 2–4 Dec 2004

Peiris N, Free M, Lubkowski Z, Hussein AT (2006) Seismic hazard and seismic design requirements for the Arabian Gulf region. First European Conference on Earthquake Engineering and Seismology, Geneva, Switzerland

Peyret DY, Hessami K, Regard V, Bellier P, Vernant P, Daigni'eres M, Nankali H, Van Gorp S, Goudarzi M, Ch′ery J, Bayer R, Rigoulay M (2009) Present-day strain distribution across the Minab-Zendan-Palami fault system from dense GPS transects. Geophys J Int 179:751–762

Plafker G, Agar R, Asker AH, Hanif M (1987) Surface effect and tectonic setting of the 13 December 1982 North Yemen earthquake. Bull Seismol Soc Am 77:2018–2037

Platt JP, Leggett JK, Alam S (1988) Slip vectors and fault mechanics in the Makran accretionary wedge, southwest Pakistan. J Geophys Res 93:7955–7973

Quittmeyer RC (1979) Seismicity variations in the Makran region of Pakistan and Iran: relation to great earthquakes. Pure Appl Geophys 117:1212–1228

Quittmeyer RC, Kafka AL (1984) Constraints on plate motions in southern Pakistan and the northern Arabian Sea from the focal mechanisms of small earthquakes. J Geophys Res 89:2444–2458

Reilinger R, McClusky S, Vernant P, Lawrence S, Ergentav S, Cakmak R, Ozener H, Kadirov F, Guliev I, Stepanyan R, Nadariya M, Hahubia G, Mahmoud S, Sakr K, ArRajehi A, Paradissis D, Al-Aydrus A, Prilepin M, Guseva T, Evren E, Dmitrotsa A, Filikov SV, Gomez F, Al-Ghazzi R, Karam G (2006) GPS constraints on continental deformation in the Africa-Arabia-Eurasia continental collision zone and implications for the dynamics of plate interactions. J Geophys Res 111:B05411

Reiter L (1990) Earthquake hazard analysis. Columbia University Press, Columbia

Rodgers A, Fowler A, Al-Amri A, Al-Enezi A (2006) The March 11, 2002 Masafi United Arab Emirates earthquake: insights into the seismotectonics of the northern Oman Mountains. Teconophys. 415:57–64

Schluter HU, Prexl A, Gaedicke C, Roeser H, Reichert C, Meyer H, Von Daniels C (2002) The Makran accretionary wedge: sediment thicknesses and ages and the origin of mud volcanoes. Mar Geol 185:219–227

Shearman DJ (1977) The geological evolution of Southern Iran, the report of the Iranian Makran expedition. Geography J 142:393–410

Slemmon DB (1977) State of the art for assessing earthquake hazard in the United States. Report 6; faults and earthquake magnitude: US Army corps of engineers, waterways experiment station, Vicksburg, Mississippi, Miscellaneous Paper S-73-1, 129

Slemmon DB (1982) Determination of design earthquake magnitude for microzonation. Third International Earthquake Microzonation Conference proceedings 1:119–130

Stafford PJ, Strasser FO, Bommer JJ (2008) An evaluation of the applicability of the NGA models to ground-motion prediction in the Euro Mediterranean region. Bull Earthq Eng 6:149–177

Stepp JC (1972) Analysis of the completeness of the earthquake sample in the Puget Sound area and its effect on statistical estimates of earthquake hazard. Proceedings of the International Conference on Microzonation for Safer Construction: Research and Application, Seattle, USA 2:897–909

Stoneley R (1974) Evolution of the continental margins bounding a former Tethys. In: Burk CA, Drake CL (eds) The geology of continental margins. Springer, New York, pp 889–903

Sykes LR, Landisman N (1964) The seismicity of East Africa, the Gulf of Aden and the Arabian and the Red Seas. Bull Seismol Soc Am 54:1927–1940

Talebian M, Jackson J (2004) A reappraisal of earthquake focal mechanisms and active shortening in the Zagros mountains of Iran. Geophys J Int 156:506–526

Vernant Ph, Nilforoushan F, Hatzfeld D, Abassi MR, Vigny C, Masson F, Nankali H, Martinod J, Ashtiani A, Bayer R, Tavakoli F, Chery J (2004) Present-day crustal deformation and plate kinematics in Middle East constrained by GPS measurements in Iran and northern Oman. Geophys J Int 157:381–398

Vita-Finzi C (2001) Neotectonics at the Arabian plate margins. J Struct Geol 23:521–530

Walker RT, Andalibi MJ, Gheitanchi MR, Jackson JA, Karegar S, Prietley K (2005) Seismological and field observationsfrom the 1990 November 6 Furg, Hormozgan, earthquake, a rare case of surface rupture in the Zagros Mountains of Iran. Geophys J Int 163:567–579

Weichert DH (1980) Estimation of the earthquakes recurrence parameters for unequal observation periods for different magnitudes. Bull Seismol Soc Am 70:1337–1346

Wells DL, Coppersmith KJ (1994) New empirical relationships among magnitude, rupture length, rupture width, rupture area, and surface displacement. Bull Seismol Soc Am 84:974–1002

Wiemer S, Giardini D, Fah D, Deichmann N, Sellami S (2008) Probabilistic seismic hazard assessment of Switzerland: best estimates and uncertainties. J Seismol 13:449–478

Yamini-Fard F, Hatzfeld D, Farahbod AM, Paul A, Mokhtari M (2007) The diffuse transition between the Zagros continental collision and the Makran oceanic subduction (Iran): microearthquake seismicity and crustal structure. Geophys J Int 170:182–194

Youngs RR, Coppersmith KJ (1985) Implications of fault slip rates and earthquake recurrence models to probabilistic seismic hazard estimates. Bull Seismol Soc Am 75:939–964

Youngs RR, Chiou SJ, Silva WJ, Humphrey JR (1997) Strong ground motion attenuation relationships for subduction zone earthquakes. Seismol Res Lett 68:58–73